processes

MDPI

Article

Green Process for the Synthesis of 3-Amino-2-methyl -quinazolin-4(3*H*)-one Synthones and Amides Thereof:DNA Photo-Disruptive and Molecular Docking Studies

Chrysoula Mikra [1,†], Maria Bairaktari [2,3,†], Marina-Theodora Petridi [2], Anastasia Detsi [2,*] and Konstantina C. Fylaktakidou [1,3,*]

1 Laboratory of Organic Chemistry, Chemistry Department, Aristotle University of Thessaloniki, 54124 Thessaloniki, Greece; chrmikgeo@chem.auth.gr
2 Laboratory of Organic Chemistry, School of Chemical Engineering, National Technical University of Athens, 15780 Athens, Greece; maro.bairakt@gmail.com (M.B.); marinapet97@gmail.com (M.-T.P.)
3 Laboratory of Organic, Bioorganic and Natural Product Chemistry, Molecular Biology and Genetics Department, Democritus University of Thrace, Dragana, 68100 Alexandroupolis, Greece
* Correspondence: adetsi@chemeng.ntua.gr (A.D.); kfylakta@chem.auth.gr (K.C.F.)
† These authors contributed equally to this work.

Abstract: Eleven 3-amino-2-methyl-quinazolin-4(3*H*)-ones have been synthesized, in good to excellent yields, via their corresponding benzoxazinones using an efficient tandem microwave-assisted green process. Representative acetamides have been thermally derived from their functional free 3-amino group, whereas for the synthesis of various arylamides, a novel green microwave-assisted protocol has been developed, which involved the attack of hydrazides on benzoxazinones. Eight out of the eleven 3-amino-2-methyl-quinazolin-4(3*H*)-ones were found photo-active towards plasmid DNA under UVB, and four under UVA irradiation. Amongst all acetamides, only the 6-nitro derivative retained activity both under UVB and UVA irradiation, whereas the 6-bromo-substituted one was active only under UVB. 3-arylamido-6-bromo derivatives exhibited dramatically decreased photo-activity; however, all 3-arylamido-6-nitro compounds developed extraordinary activity, even at concentrations as low as 1μM, which was enhanced compared to their parent 3-amino-2-methyl-6-nitro-quinazolinone. Molecular docking studies were indicative of satisfactory binding to DNA and correlated to the presented photo-activity. Since quinazolinones are known "privileged" pharmacophores for anticancer and antimicrobial activities, the present study gives information on turning "on" and "off" photosensitization on various derivatives which are often used as synthones for drug development, when chromophores and auxochromes are incorporated or being functionalized. Thus, certain compounds may lead to the development of novel photo-chemo or photodynamic therapeutics.

Keywords: privileged structures; microwave-assisted synthesis; benzoxazinones; 3-Amino-quinazolin-4(3*H*)-ones; 3-Arylamido-quinazolin-4(3*H*)-ones; 6-Nitro-Quinazolinone; DNA photocleavers; photodynamic effects; aerobic and anaerobic DNA photo-cleavage; molecular docking

Citation: Mikra, C.; Bairaktari, M.; Petridi, M.-T.; Detsi, A.; Fylaktakidou, K.C. Green Process for the Synthesis of 3-Amino-2-methyl-quinazolin-4(3*H*)-one Synthones and Amides Thereof:DNA Photo-Disruptive and Molecular Docking Studies. *Processes* **2022**, *10*, 384. https://doi.org/10.3390/pr10020384

Academic Editor: Alina Bora

Received: 10 January 2022
Accepted: 11 February 2022
Published: 17 February 2022

1. Introduction

Quinazolinones belong to a class of heterocyclic compounds found in numerous natural products [1,2]. Structurally, the bi-cyclic frame of quinazolin-4(3*H*)-ones (QNZs), (Figure 1**I**) consists of an aromatic ring with four positions available for derivatization, as well as a fused heterocyclic ring holding two nitrogen atoms and a carbonyl group in the form of an amide. Those functionalities provide an internal network for the creation of intermolecular forces—most probably valuable for their communication with biological domains—and opportunities for further synthetically-derived diversity. The relatively easy way to synthesize QNZs, from cheap and commercially available reagents, such as *o*-amino-benzonitriles, substituted anthranilic acids and esters, benzamides, *o*-amino-halobenzene,

etc, using both conventional or green methodologies and their ability to exhibit affinities with diverse biological targets, renders this class of compounds to become "privileged" in medicinal chemistry [3–5]. Among the plethora of synthetic derivatives, a number of studies indicate halogenated derivatives (most commonly, Br and I at positions 6-, [6–11] or 7- [12] and 6,8- [13,14]) as promising lead compounds, mainly for antimicrobial, as well as anticancer, drugs for future development. Lately, the combination of the QNZ pharmacophore in the form of a hybrid with other bioactive compounds has gained more ground [4], whereas their technical use as molecular platforms for luminescence materials and bioimaging agents is emerging [15].

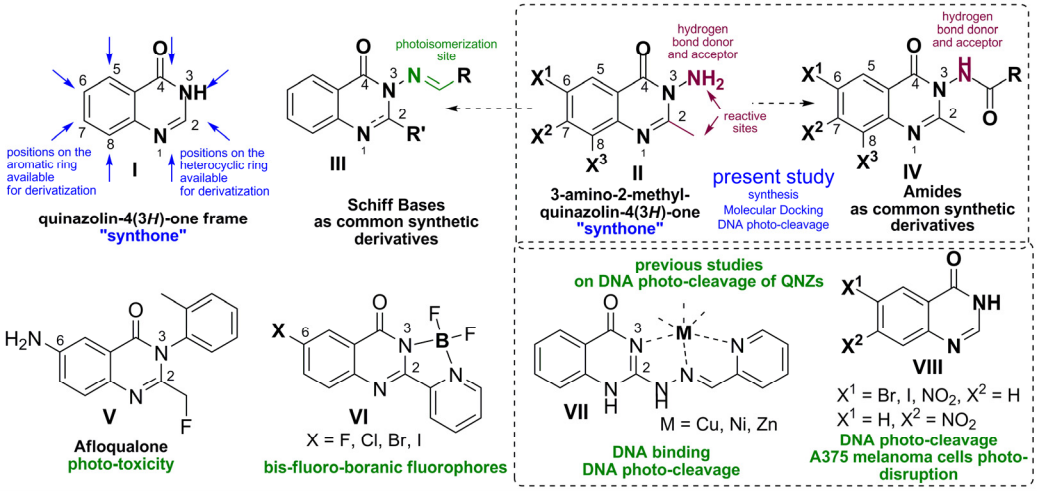

Figure 1. Structures of quinazolin-4(3*H*)-one and 3-amino-2-methyl quinazolin-4(3*H*)-one as synthones (**I** and **II**, respectively); Common general structures of synthetic compounds derived from the amine functionality (**III** and **IV**, respectively); Compounds found in the literature to show photoisomerization (**III**), phototoxicity (**V**), fluorescence activity (**VI**) and DNA photo-cleavage (**VII**, **VIII**).

Among the variety of derivatives, 3-amino-2-methyl-QNZs which bear the amine functional group attached on the 3-nitrogen and a reactive methyl group linked on the skeletal carbon atom of the heterocyclic part (Figure 1**II**), represents a class of synthones, an "intermediate compound" that allows a variety of groups, aromatic and heteroaromatic moieties to be linked or attached on the quinazolinone heterocyclic ring usually in the form of a Schiff base or an amide (Figure 1**IV**, respectively). Indeed, diverse bioactive QNZ derivatives bearing benzoxazepine [16], urea and thiourea derivatives [17,18], 2,3- [19] and 3,4-fused [20] heterocyclic systems, sulfonamides [21], 1,3,5-triazines [6,22], oxadiazoles [23], and others [24] have been investigated. Additionally, the methyl group easily provides extension to alkene (more specifically, 2-arylethylene) functionalities via dehydration reactions with aldehydes [25], whereas, both amine and methyl groups may participate in reactions leading to tricyclic [19] or polycyclic heterocyclic compounds with applications in polymer chemistry and dye industry [26,27].

The QNZ core frame was found non-photo-responding [28], and, in general, studies on this direction are rather scarce. Photo-stability of drugs is important in order to avoid side effects related to phototoxicity; on the other hand, as different sides of the same coin, photosensitivity is required for spatially and temporally controlled, alternative, non-invasive, photo-therapeutic applications, in various cancer treatment protocols [29,30], and inactivation of bacteria. Especially for microbial photo-inactivation, scientists tend to believe that the extensive caused damage give bacteria limited potential to develop resistance [31–33]. Research concerning non-porphyroid derivatives [34] as well as oxygen independent mechanisms of action [35] are of great interest. In the literature, syn–anti-photoisomerization of 2-arylethylene [36,37], or 3-aryl-imino (Schiff bases) [38] QNZ derivatives (Figure 1, certain compounds under the general structure **III**) were found to be photochemically activatable, with the activation site located outside of the QNZ frame. Checking photoactivation

caused by various fragments attached on QNZs, one may notice that the central nervous acting muscle relaxant commercial drug "Afloqualone (AFQ)" [39], (Figure 1**V**), caused photosensitive skin reactions. More experimentation revealed that the drug was phototoxic to bacteriophage lambda [40], while it was exhibiting DNA photo-cleavage activity by photodynamic action [41,42].

In the direction of molecular imaging, the so called "heavy atom effect" has been applied in the synthesis of 6-halogenated QNZ bis-fluoro-boranic fluorophores with high Stokes shifts and high fluorescence quantum yields, (Figure 1**VI**) [43]. Incorporation of metal coordination in properly designed QNZs (Figure 1**VII**) and quinazoline Schiff bases, bearing no substituents on the aromatic ring, led to the appearance of photosensitivity with photodynamic mechanisms [44,45]. Whereas not all examined metal complexes exhibited photo-reactivity both ligands and metal complexes showed DNA-binding and/or DNA cleaving in dark and under irradiation [46,47]. Other examples of DNA binding and cleaving QNZ agents exist in the literature [48,49].

It seems that the properties or the positioning of certain substituents on the QNZ scaffold introduce ability for photosensitization on this important class of compounds. Driven by these observations, we have initiated an investigation of a possible photo-activation towards DNA of QNZ derivatives bearing very common atoms and groups on their skeleton (Figure 1**VIII**). We have found that the existence of Br and I atoms in position 6- of the frame lead to the homolysis of the C-halogen bond under UV-B irradiation, whereas the nitro group was leading to DNA photo-cleavage and photo-degradation of A-375 metastatic melanoma cells under UV-A irradiation [50].

In the present study, we wish to present our findings in the photo-reactivity of 3-amino-2-methyl-QNZs (Figure 1**II**) towards DNA. The incorporated amine functionality attached to the nitrogen at position 3- of QNZ introduces an extra hydrogen bond participant, which in combination with a variety of substituents on the aromatic ring may altogether alter physicochemical characteristics and affect both light absorption as well as affinity to DNA. Those features set up the basis for the photo-biological behaviour of 3-amino-QNZ synthones. Partial alteration of the hydrogen bond capacity of the amine by converting it into amides (Figure 1**IV**) with the insertion of an acetyl or an aroyl group allows a second level of structure activity relationship study. Microwave irradiation (MWI) assisted green synthesis has been attempted for almost all reactions.

In order to investigate the photo-disrupting activity of the compounds towards DNA, the experimental approach utilized the photo-cleavage of a plasmid DNA as a useful and multi-informative sensitive marker which "senses" compounds with biological interest vulnerable to photoexcitation, under irradiation at wavelengths over 300 nm that are transparent to biological molecules. In addition to photo-cleavage and mechanism of action, this experiment may identify DNA-binders, which is a requirement for photo-cleavage [51–54]. The study was completed with DNA Molecular docking theoretical studies.

2. Materials and Methods

All commercially available reagent-grade chemicals and solvents were used without further purification. pB322 supercoiled plasmid was purchased from New England Biolabs. UV-visible (UV-vis) spectra were recorded in solution at concentrations in the range 10 μM-5 mM on Hitachi U-2001 dual beam or JASCO V-770 UV-Vis/NIR spectrophotometers. NMR spectra were recorded on Agilent 500/54 (500 MHz and 125 MHz for ^{1}H and ^{13}C, respectively) or Varian 600 MHz (Institute of Chemical Biology of National Hellenic Research Foundation) spectrometers using $CDCl_3$, and/or DMSO-*d6* as solvent. *J* values are reported in Hz. Infrared (IR) spectra were recorded in the range 400–4000 cm^{-1} on Nicolet FT-IR 6700 or JASCO FT/IR-4200 spectrometers with samples prepared as KBr pellets. Mass spectra were determined using a Shimadzu LCMS-2010 EV system under electrospray ionization (ESI) conditions. The High-Resolution Mass Spectra measured with a Q-TOF (Time of Flight Mass Spectrometry) Bruker Maxis Impact with ESI source and

U-HPLC Thermo Dionex Ultimate 3000 pump and autosampler. N_2 was used as collision gas and electrospray ionization (ESI) was used for the MS experiments. The data acquisition was carried out with Data analysis from Bruker Daltonics (version 4.1). All samples containing pBR322 plasmid were irradiated at pH 6.8 with Philips 2 × 9W/01/2P UV-B narrowband lamps at 312 nm, Philips 2 × 9W/10/2P UV-A broad band lamps at 365 nm, or white light OSRAM DULUX S BLUE. MW experiments were performed on Biotage Initiator 2.0 or Milestone StartSynth Microwave Reactors. All reactions were monitored on commercially available pre-coated TLC plates (layer thickness 0.25 mm) of Kieselgel 60 F_{254}. Melting points were measured on a Kofler hot-stage or a GallenKamp MFB-595 melting point apparatuses and are uncorrected. Calculation of yields was based on the amount of the crystallized product.

2.1. Synthesis of Chemical Compounds

2.1.1. General Method for the Synthesis of Benzoxazinones (**2a**-**2k**)

A mixture of substituted anthranilic acid (3 mmol) and acetic anhydride (5 mL) was added in a microwave tube (thermowell) and the mixture was heated under MWI at 250 W for 17–22 min at a fixed temperature (120–150 °C). The reaction mixture was cooled, a precipitate appeared and was filtered, washed with petroleum ether and dried to produce the desired BZNs, which was used in the next step without any further purification.

2.1.2. General Method for the Synthesis of Substituted 2-methyl-3-amino–quinazolin -4(3H) ones (**3a**-**3k**)

To a solution of each individual BZN **2a**-**2k** (1 mmol) in 5 mL of absolute ethanol, hydrazine monohydrate (3 mmol) was added in a microwave tube and the mixture was irradiated under MWI at 250 W for 20–33 min at a fixed temperature (120–150 °C). After cooling and distilling off most of the solvent in a rotary evaporator a solid was formed which was filtered off and recrystallized from appropriate solvent to produce the desired compounds in 31–85% yield, over two steps. UV-Vis spectra have been recorded in MeOH (10^{-2} mg/mL) and from 250–500 nm.

- 3-amino-6-hydroxy-2-methylquinazolin-4(3*H*)-one (**3a**) [26]: Off white amorphous solid; mp: 294–296 °C; yield: 32%; ^{1}H-NMR (DMSO-d_6, 600 MHz): δ (ppm) 9.98 (s,1H, OH), 7.46 (d, J = 8.4 Hz, 1H, H_8), 7.36 (d, J = 1.8 Hz, 1H, H_5), 7.23 (dd, J = 8.4, 1.8 Hz, 1H, H_7), 5.75 (s, 2H, NH_2), 2.52 (s, 3H, CH_3); UV-Vis (e $M^{-1}cm^{-1}$): λ (nm) = 274 (11,854), 329 (4780).
- 3-amino-2,6-dimethylquinazolin-4(3*H*)-one (**3b**) [55]: White amorphous solid; mp: 170–171 °C; yield: 31%; ^{1}H-NMR (DMSO-d_6, 600 MHz): δ (ppm) 7.89 (s, 1H, H_5), 7.60 (d, J = 7.8, 1.8 Hz, 1H, H_7), 7.50 (d, J = 7.8 Hz, 1H, H_8), 5.78 (s, 2H, NH_2), 2.56 (s, 3H, CH_3), 2.44 (s, 3H, CH_3); UV-Vis (e $M^{-1}cm^{-1}$): λ (nm) = 271 (5482), 312 (2268).
- 3-amino-2-methylquinazolin-4(3*H*)-one (**3c**) [56]: White amorphous solid; mp: 142–143 °C; yield: 35%; ^{1}H-NMR ($CDCl_3$, 300 MHz): δ (ppm) 8.08 (d, 1H, H_5), 7.63–7.61 (m, 2H), 7.36–7.31 (m, 1H), 5.15 (s, 2H, NH_2), 2.66 (s, 3H, CH_3); UV-Vis (e $M^{-1}cm^{-1}$): λ (nm) = 273 (684).
- 3-amino-6-fluoro-2-methylquinazolin-4(3*H*)-one (**3d**) [57]: White amorphous solid; mp: 198–199 °C; yield: 51%; ^{1}H-NMR (DMSO-d_6, 600 MHz): δ (ppm) 7.76 (dd, J = 8.16, 1.6 Hz, 1H, H_7), 7.68–7.66 (m, 2H, H_5, H_8), 5.82 (s, 2H, NH_2), 2.57 (s, 3H, CH_3); UV-Vis (e $M^{-1}cm^{-1}$): λ (nm) = 265 (6178), 314 (3475).
- 3-amino-6-chloro-2-methylquinazolin-4(3*H*)-one (**3e**) [58]: White amorphous solid; mp: 174–175 °C; yield: 50%; ^{1}H-NMR (DMSO-d_6, 600 MHz): δ (ppm) 8.03 (d, J = 2.3 Hz, 1H, H_5), 7.80 (dd, J = 8.7, 2.4 Hz, 1H, H_7), 7.63 (d, J = 8.76 Hz, 1H, H_8), 5.84 (s, 2H, NH_2), 2.58 (s, 3H, CH_3); UV-Vis (e $M^{-1}cm^{-1}$): λ (nm) = 274 (8996), 316 (3347).
- 3-amino-7-chloro-2-methylquinazolin-4(3*H*)-one (**3f**) [59]: White amorphous solid; mp: 197–200 °C; yield: 40%; ^{1}H-NMR (DMSO-d_6, 600 MHz): δ (ppm) 8.09 (d, J = 8.5 Hz, 1H, H_5), 7.39 (d, J = 1.6 Hz, 1H, H_8), 7.50 (dd, J = 8.5, 1.8 Hz, 1H, H_6), 5.81 (s, 2H, NH_2), 2.58 (s, 3H, CH_3); UV-Vis (e $M^{-1}cm^{-1}$): λ (nm) = 278 (5439).

- 3-amino-6-bromo-2-methylquinazolin-4(3*H*)-one (**3g**) [11]: Pale yellow amorphous solid; mp: 187–189 °C; yield: 70%; ^{1}H-NMR (DMSO-d_6, 600 MHz): δ (ppm) 8.15 (s, 1H, H_5), 7.89 (dd, J = 8.4 Hz, 1H, H_7), 7.53 (d, J = 8.6, 1H, H_8), 5.83 (s, 2H, NH_2), 2.57(s, 3H, CH_3); UV-Vis (e $M^{-1}cm^{-1}$): λ (nm) = 283 (15,000), 316 (8000).
- 3-amino-6,8-dibromo-2-methylquinazolin-4(3*H*)-one (**3h**) [60]: Yellow amorphous solid; mp: 231–232 °C; yield: 85%; ^{1}H-NMR (DMSO-d_6, 300 MHz): δ (ppm) 8.31 (d, J = 2.2 Hz, 1H, H_7), 8.18 (d, J = 2.2 Hz, 1H, H_5), 5.88 (s, 2H, NH_2), 2.61 (s, 3H, CH_3); UV-Vis (e $M^{-1}cm^{-1}$): λ (nm) = 286 (7285).
- 3-amino-6-iodo-2-methylquinazolin-4(3*H*)-one (**3i**) [61]: Off white amorphous solid; mp: 186–187 °C; yield: 63%; ^{1}H-NMR (DMSO-d_6, 600 MHz): δ (ppm) 8.36 (d, J = 2.1 Hz, 1H, H_5), 8.04 (dd, J = 8.6, 2.1 Hz, 1H, H_7), 7.39 (d, J = 8.6 Hz, 1H, H_8), 5.82 (s, 2H, NH_2), 2.56 (s, 3H, CH_3); UV-Vis (e $M^{-1}cm^{-1}$): λ (nm) = 279 (13,253).
- 3-amino-2-methyl-6-nitroquinazolin-4(3*H*)-one (**3j**) [27]: Yellow amorphous solid; mp: 178–180 °C; yield: 85%; ^{1}H-NMR (DMSO–d_6, 600 MHz): δ (ppm) 8.80 (d, J = 2.3 Hz, 1H, H_5), 8.49 (dd, J = 9.0, 2.4 Hz, 1H, H_7), 7.78 (d, J = 8.9 Hz, 1H, H_8), 5.92 (s, 2H, NH_2), 2.64 (s, 3H, CH_3); UV-Vis (e $M^{-1}cm^{-1}$): λ (nm) = 326 (9692).
- 3-amino-2-methyl-7-nitroquinazolin-4(3*H*)-one (**3k**) [62]: Yellow amorphous solid; mp: 218–219 °C; yield: 48%; ^{1}H-NMR (DMSO-d_6, 600 MHz): δ (ppm) 8.32 (m, 2H, H_5, H_8), 8.19 (dd, J = 8.64, 1.98 Hz, 1H, H_6), 5.92 (s, 2H, NH_2), 2.63 (s, 3H, CH_3); UV-Vis (e $M^{-1}cm^{-1}$): λ (nm) = 258 (18,502), 344 (1762).

2.1.3. General Method of Synthesis of Acetamides (**4**–**8**)

To the solution of **3** (1 mmol) in dry toluene (5 mL), acetyl chloride (2 mmol) was added drop by drop at 110 °C and the reaction mixture was stirred overnight. The excess solvent was distilled under reduced pressure and then poured into ice. The solid thus obtained was recrystallized from ethanol. UV-vis spectra were recorded in DMSO (10^{-4} M) and from 250–500 nm.

- *N*-(2-methyl-4-oxoquinazolin-3(4*H*)-yl)acetamide (**4**) [63]: White amorphous solid; mp: 224–226 °C; yield: 87%; ^{1}H NMR ($CDCl_3$, 300 MHz): δ (ppm) 8.80 (s, 1H, NHCO), 8.19 (d, J = 7.8 Hz, 1H, H_5), 7.76 (t, J = 8.1 Hz, 1H), 7.65 (d, J = 8.4Hz, 1H), 7.45 (t, J = 7.5 Hz, 1H), 2.54 (s, 3H, CH_3), 2.26 (s, 3H, CH_3); UV-Vis (e $M^{-1}cm^{-1}$): λ (nm) = 271 (12,200), 305 (7100).
- *N*-(6-chloro-2-methyl-4-oxoquinazolin-3(4*H*)-yl)acetamide (**5**): White amorphous solid; mp: 206–208 °C; yield: 45%; MS(ESI) m/z $[M]^+$: 252; ^{1}H NMR (DMSO-d_6, 500 MHz): δ (ppm) 11.09 (s, 1H, NHCO), 8.04 (d, J = 2.4 Hz, 1H, H_5), 7.88 (dd, J = 8.8, 2.5 Hz, 1H, H_7), 7.67 (d, J = 8.7 Hz, 1H, H_8), 2.38 (s, 3H, CH_3), 2.11 (s, 3H, CH_3); ^{13}C-NMR (DMSO-d_6, 125 MHz) δ 169.1, 158.0, 156.8, 145.3, 135.1, 130.9, 129.2, 125.3, 121.9, 21.1, 20.4; UV-Vis (e $M^{-1}cm^{-1}$): λ (nm) = 277 (14,300), 315 (6200).
- *N*-(6-bromo-2-methyl-4-oxoquinazolin-3(4*H*)-yl)acetamide (**6**) [63]: Off white amorphous solid; mp: 228–230 °C; yield: 49%; ^{1}H NMR (DMSO-d_6, 500 MHz): δ (ppm) 11.09 (s, 1H, NHCO), 8.17 (d, J = 2.3 Hz, 1H, H_5), 7.99 (dd, J = 8.7, 2.3 Hz, 1H, H_7), 7.59 (d, J = 8.7 Hz, 1H, H_8), 2.37 (s, 3H, CH_3), 2.11 (s, 3H, CH_3); ^{13}C-NMR (DMSO-d_6, 125 MHz) δ 162.1, 157.8, 157.0, 145.6, 137.8, 129.3, 128.4, 122.2, 119.0, 21.1, 20.5; UV-Vis (e $M^{-1}cm^{-1}$): λ (nm) = 280 (15,200), 315 (7200).
- *N*-(6-iodo-2-methyl-4-oxoquinazolin-3(4*H*)-yl)acetamide (**7**): Beige amorphous solid; mp: 182–184 °C; yield: 42%; MS(ESI) m/z $[M]^+$: 344; ^{1}H NMR (DMSO-d_6, 500 MHz): δ (ppm) 11.07 (s, 1H, NHCO), 8.35 (d, J = 2.0 Hz, 1H, H_5), 8.12 (dd, J = 8.6, 2.0 Hz, 1H, H_7), 7.42 (d, J = 8.6 Hz, 1H, H_8), 2.36 (s, 3H, CH_3), 2.10 (s, 3H, CH_3); ^{13}C-NMR (DMSO-d_6, 125 MHz) δ 169.1, 157.7, 157.0, 145.9, 143.3, 134.5, 129.1, 122.4, 91.6, 21.1, 20.5; UV-Vis (e $M^{-1}cm^{-1}$): λ (nm) = 286 (15,800), 318 (6000).
- *N*-(2-methyl-6-nitro-4-oxoquinazolin-3(4*H*)-yl)acetamide (**8**): Yellow amorphous solid; mp: 242–244 °C; yield: 76%; MS(ESI) m/z $[M]^+$: 263; ^{1}H NMR (DMSO-d_6, 500 MHz): δ (ppm) 11.21 (s, 1H, NHCO), 8.78 (d, J = 2.6 Hz, 1H, H_5), 8.58 (dd, J = 9.0, 2.7 Hz,

1H, H_7), 7.84 (d, *J* = 9.0 Hz, 1H, H_8), 2.45 (s, 3H, CH_3), 2.13 (s, 3H, CH_3); ^{13}C-NMR (DMSO-d_6, 125 MHz) δ 169.2, 160.2, 158.2, 150.6, 145.0, 129.0, 128.8, 122.5, 120.7, 21.4, 20.4; UV-Vis (e $M^{-1}cm^{-1}$): λ (nm) = 270 (11,000), 318 (15,300), 329 (15,000).

2.1.4. General Method of Synthesis of Arylamides (**9**–**19**)

To a solution of **2c**, or **2g**, or **2j** (1 mmol) in acetic acid (1 mL), the corresponding arylhydrazide (1 mmol) was added and the mixture was heated under MWI at 150 °C for 30 min. Upon cooling down, water was added, and the precipitate was filtered to obtain the desired compounds at 58–87% yield. Crude samples showed high purity by ^{1}H-NMR. Recrystallization was performed in order to provide m.p. and solvent of recrystallization of all compounds. UV-vis spectra were recorded in DMSO (10^{-4} M) and from 250−500 nm. For compound **9** c = 5 × 10^{-4} M and for compound **10** c = 2.5 × 10^{-4} M.

- 4-chloro-*N*-(2-methyl-4-oxoquinazolin-3(4*H*)-yl)benzamide (**9**) [64]: White amorphous solid; mp: 238–240 °C; yield: 72%; IR (KBr): 3234, 1704, 1667, 1606 cm^{-1}; ^{1}H-NMR (DMSO-d_6, 500 MHz) δ 11.76 (brs, 1H, NHCO), 8.13 (d, *J* = 7.8 Hz, 1H), 8.02 (d, *J* = 8.4 Hz, 2H), 7.88 (t, *J* = 8.1 Hz, 1H), 7.69 (dd, *J* = 8.5, 2.1 Hz, 2H), 7.56 (t, *J* = 7.6 Hz, 1H), 2.46 (s, 3H, CH_3) ppm; ^{13}C-NMR (DMSO-d_6, 125 MHz,) δ 165.0, 159.0, 156.1, 146.6, 137.7, 135.1, 130.0, 129.7, 129.0, 127.0, 126.9, 126.5, 120.6, 21.0 ppm; UV-Vis (e $M^{-1}cm^{-1}$): λ (nm) = 273 (3600), 305 (1600); HRMS(ESI) *m*/*z* [M+Na]$^+$: $C_{16}H_{12}ClN_3NaO_2^+$, calc: 336.0510; found: 336.0510.
- *N*-(2-methyl-4-oxoquinazolin-3(4*H*)-yl)-4-nitrobenzamide (**10**) [64]: Beige amorphous solid; mp: 269–272 °C; yield: 60%; IR (KBr): 3215, 1701, 1662, 1605 cm^{-1}; ^{1}H-NMR (DMSO-d_6, 500 MHz) δ 12.04 (s, 1H, NHCO), 8.46 (d, *J* = 8.9 Hz, 2H), 8.25 (d, *J* = 8.9 Hz, 2H), 8.15 (dd, *J* = 7.9, 1.0 Hz, 1H), 7.91 (dt, *J* = 8.4, 1.4 Hz, 1H), 7.71 (d, *J* = 8 Hz, 1H), 7.58 (t, *J* = 7.9 Hz, 1H), 2.50 (s, 3H, CH_3) ppm; ^{13}C-NMR (DMSO-d_6, 125 MHz,) δ 165.3, 159.4, 156.5, 150.4, 146.8, 137.1, 135.9, 129.8, 127.6, 127.3, 127.0, 124.5, 120.8, 21.4 ppm; UV-Vis (e $M^{-1}cm^{-1}$): λ (nm) = 275 (7040), broad declining shoulder up to ~340 nm; HRMS(ESI) *m*/*z* [M+H]$^+$: $C_{16}H_{13}N_4O_4^+$, calc: 325.0931; found: 325.0930.
- 4-methoxy-*N*-(2-methyl-4-oxoquinazolin-3(4*H*)-yl)benzamide (**11**) [65]: White amorphous solid; mp: 193–195 °C; yield: 82%; IR (KBr): 3215, 1702, 1659, 1608 cm^{-1}; ^{1}H-NMR (DMSO-d_6, 500 MHz) δ 11.47 (s, 1H, NHCO), 8.12 (d, *J* = 7.8 Hz, 1H), 7.98 (d, *J* = 8.7 Hz, 2H), 7.88 (t, *J* = 8.1 Hz, 1H), 7.68 (d, *J* = 8.1 Hz, 1H), 7.56 (t, *J* = 7.4 Hz, 1H), 7.13 (d, *J* = 8.7 Hz, 2H), 3.87 (s, 3H, OCH_3), 2.44 (s, 3H, CH_3) ppm; ^{13}C-NMR (DMSO-d_6, 125 MHz,) δ 165.7, 163.0, 159.4, 156.7, 146.8, 135.4, 130.1, 127.1, 127.1, 126.7, 123.4, 120.8, 114.3, 55.8, 21.3 ppm; UV-Vis (e $M^{-1}cm^{-1}$): λ (nm) = 274 (18,000), 305 (5500); HRMS(ESI) *m*/*z* [M+Na]$^+$: $C_{17}H_{15}N_3NaO_3^+$, calc: 332.1006; found: 332.1003.
- *N*-(6-bromo-2-methyl-4-oxoquinazolin-3(4*H*)-yl)-4-chlorobenzamide (**12**): Off white amorphous solid; mp: 275–277 °C (EA+EtOH); yield: 76%; IR (KBr): 3263, 1698, 1668, 1603 cm^{-1}; ^{1}H-NMR (DMSO-d_6, 500 MHz) δ 11.82 (s, 1H, NHCO), 8.21 (d, *J* = 2.1 Hz, 1H, H_5), 8.04 (dd, *J* = 8.8, 2.2 Hz, 1H, H_7), 8.01 (d, *J* = 8.5 Hz, 2H, ArCO), 7.69 (d, *J* = 8.5 Hz, 2H, ArCO), 7.65 (d, *J* = 8.7 Hz, 1H, H_8), 2.45 (s, 3H, CH_3) ppm; ^{13}C-NMR (DMSO-d_6, 125 MHz) δ 165.0, 157.9, 156.9, 145.6, 138.1, 137.8, 129.8, 129.8, 129.5, 129.0, 128.5, 122.2, 119.3, 21.1 ppm; UV-Vis (e $M^{-1}cm^{-1}$): λ (nm) = 274 (12,800), 315 (3800); HRMS(ESI) *m*/*z* [M+H]$^+$: $C_{16}H_{12}BrClN_3O_2^+$, calc: 391.9796; found: 391.9795.
- *N*-(6-bromo-2-methyl-4-oxoquinazolin-3(4*H*)-yl)-4-nitrobenzamide (**13**): Off white amorphous solid; yield: 65%; mp: 287–290 °C (EA+EtOH); IR (KBr): 3280, 1696, 1665, 1598 cm^{-1}; ^{1}H-NMR (DMSO-d_6, 500 MHz) δ 12.09 (s, 1H, NHCO), 8.43 (d, *J* = 8.6 Hz, 2H, ArCO), 8.21 (d, *J* = 8.1 Hz, 2H, ArCO), 8.20 (obscured, 1H, H_5), 8.03 (d, *J* = 8.8 Hz, 1H, H_7), 7.64 (d, *J* = 8.7 Hz, 1H, H_8), 2.47 (s, 3H, CH_3) ppm; ^{13}C-NMR (DMSO-d_6, 125 MHz) δ 164.5, 157.8, 156.7, 150.0, 145.6, 138.1, 136.6, 129.5, 129.4, 128.5, 124.0, 122.1, 119.4, 21.1 ppm; UV-Vis (e $M^{-1}cm^{-1}$): λ (nm) = 280 (14,100), broad declining shoulder up to ~340 nm; HRMS(ESI) *m*/*z* [M+Na]$^+$: $C_{16}H_{11}BrN_4NaO_4^+$, calc: 424.9856; found: 424.9852.

- *N*-(6-bromo-2-methyl-4-oxoquinazolin-3(4*H*)-yl)-4-methoxybenzamide (**14**): White amorphous solid; yield: 78%; mp: 215–217 °C (EA); IR (KBr): 3311, 1700, 1664, 1605 cm^{-1}; ^{1}H-NMR (DMSO-d_6, 500 MHz) δ 11.54 (s, 1H, NHCO), 8.21 (d, J = 2.1 Hz, 1H, H_5), 8.03 (dd, J = 8.7, 2.1 Hz, 1H, H_7), 7.98 (d, J = 8.7 Hz, 2H, ArCO), 7.65 (d, J = 8.7 Hz, 1H, H_8), 7.13 (d, J = 8.7 Hz, 2H, ArCO), 3.86 (s, 3H, OCH_3), 2.44 (s, 3H, CH_3) ppm; ^{13}C-NMR (DMSO-d_6, 125 MHz) δ 165.3, 162.8, 158.0, 157.2, 145.6, 137.9, 129.9, 129.4, 128.4, 123.1, 122.2, 119.2, 114.1, 55.6, 21.1 ppm; UV-Vis (e $M^{-1}cm^{-1}$): λ (nm) = 278 (14,400), 315 (3800); HRMS(ESI) m/z $[M+H]^+$: $C_{17}H_{15}BrN_3O_3^+$, calc: 388.0291; found: 388.0287.
- *N*-(6-bromo-2-methyl-4-oxoquinazolin-3(4*H*)-yl)benzamide (**15**): Off white amorphous solid; yield: 84%; mp: 265–267 °C (EA); IR (KBr): 3262, 1694, 1669, 1607 cm^{-1}; ^{1}H-NMR (DMSO-d_6, 500 MHz) δ 11.71 (s, 1H, NHCO), 8.22 (d, J = 2.2 Hz, 1H, H_5), 8.04 (dd, J = 8.6, 2.2 Hz, 1H, H_7), 8.00 (d, J = 7.3 Hz, 2H, ArCO), 7.70 (t, J = 7.5 Hz, 1H, ArCO), 7.65 (d, J = 8.7 Hz, 1H, H_8), 7.61 (t, J = 7.6 Hz, 2H, ArCO), 2.46 (s, 3H, CH_3) ppm; ^{13}C-NMR (DMSO-d_6, 125 MHz) δ 165.8, 157.9, 157.0, 145.6, 138.0, 132.9, 131.1, 129.4, 128.8, 128.4, 127.8, 122.2, 119.2, 21.1 ppm; UV-Vis (e $M^{-1}cm^{-1}$): λ (nm) = 274 (11,800), 315 (3200); HRMS(ESI) m/z $[M+H]^+$: $C_{16}H_{13}BrN_3O_2^+$, calc: 358.0186; found: 358.0178.
- 4-chloro-*N*-(2-methyl-6-nitro-4-oxoquinazolin-3(4*H*)-yl)benzamide (**16**): Pale yellow amorphous solid; yield: 58%; mp: 257–260 °C (EtOH); IR (KBr): 3273, 1705, 1681, 1601 cm^{-1}; ^{1}H-NMR (DMSO-d_6, 500 MHz) δ 11.96 (s, 1H, NHCO), 8.82 (d, J = 2.6 Hz, 1H, H_5), 8.61 (dd, J = 9.0, 2.6 Hz, 1H, H_7), 8.03 (d, J = 8.5 Hz, 2H, ArCO), 7.90 (d, J = 9.0 Hz, 1H, H_8), 7.70 (d, J = 8.5 Hz, 2H, ArCO), 2.54 (s, 3H, CH_3) ppm; ^{13}C-NMR (DMSO-d_6, 125 MHz) δ 165.0, 160.1, 158.2, 150.6, 145.1, 137.8, 129.8, 129.7, 129.2, 129.0, 129.0, 122.6, 120.6, 21.5 ppm; UV-Vis (e $M^{-1}cm^{-1}$): λ (nm) = 265 (6800), 325 (10,800); HRMS(ESI) m/z $[M+H]^+$: $C_{16}H_{12}ClN_4O_4^+$, calc: 359.0542; found: 359.0549.
- *N*-(2-methyl-6-nitro-4-oxoquinazolin-3(4*H*)-yl)-4-nitrobenzamide (**17**): Beige amorphous solid; yield: 80%; mp: 244–246 °C (EtOH); IR (KBr): 3209, 1713, 1675, 1604 cm^{-1}; ^{1}H-NMR (DMSO-d_6, 500 MHz) δ 12.24 (s, 1H, NHCO), 8.83 (d, J = 2.6 Hz, 1H, H_5), 8.63 (dd, J = 9.0, 2.7 Hz, 1H, H_7), 8.45 (d, J = 8.7 Hz, 2H, ArCO), 8.24 (d, J = 8.7 Hz, 2H, ArCO), 7.91 (d, J = 9.0 Hz, 1H, H_8), 2.56 (s, 3H, CH_3) ppm; ^{13}C-NMR (DMSO-d_6, 125 MHz) δ 164.5, 159.9, 158.0, 150.6, 150.0, 145.2, 136.5, 129.5, 129.3, 129.0, 124.0, 122.6, 120.6, 21.4 ppm; UV-Vis (e $M^{-1}cm^{-1}$): λ (nm) = 270 (12,700), 321 (12,900); HRMS(ESI) m/z $[M+Na]^+$: $C_{16}H_{11}N_5NaO_6^+$, calc: 392.0602; found: 392.0604.
- 4-methoxy-*N*-(2-methyl-6-nitro-4-oxoquinazolin-3(4*H*)-yl)benzamide (**18**): Beige amorphous solid; yield: 84%; mp: 228–230 °C (EtOH); IR (KBr): 3306, 1699, 1678, 1606 cm^{-1}; ^{1}H-NMR (DMSO-d_6, 500 MHz) δ 11.67 (s, 1H, NHCO), 8.81 (d, J = 2.6 Hz, 1H, H_5), 8.61 (dd, J = 8.9, 2.6 Hz, 1H, H_7), 8.00 (d, J = 8.8 Hz, 2H, ArCO), 7.90 (d, J = 9.0 Hz, 1H, H_8), 7.14 (d, J = 8.7 Hz, 2H, ArCO), 3.87 (s, 3H, OCH_3), 2.52 (s, 3H, CH_3) ppm; ^{13}C-NMR (DMSO-d_6, 125 MHz) δ 165.4, 163.0, 160.4, 158.4, 150.7, 145.1, 130.0, 129.2, 129.0, 123.0, 122.7, 120.7, 114.2, 55.6, 21.5 ppm; UV-Vis (e $M^{-1}cm^{-1}$): λ (nm) = 269 (11,200), 326 (10,900); HRMS(ESI) m/z $[M+Na]^+$: $C_{17}H_{14}N_4NaO_5^+$, calc: 377.0856; found: 377.0856.
- *N*-(2-methyl-6-nitro-4-oxoquinazolin-3(4*H*)-yl)benzamide (**19**): Off white amorphous solid; yield: 87%; mp: 262–264 °C (EtOH); IR (KBr): 3271, 1690, 1678, 1603 cm^{-1}; ^{1}H-NMR (DMSO-d_6, 500 MHz) δ 11.85 (s, 1H, NHCO), 8.82 (d, J = 2.6 Hz, 1H, H_5), 8.62 (dd, J = 8.9, 2.7 Hz, 1H, H_7), 8.01 (d, J = 7.2 Hz, 2H, ArCO), 7.90 (d, J = 9.0 Hz, 1H, H_8), 7.71 (t, J = 7.5 Hz, 1H, ArCO), 7.62 (t, J = 7.7 Hz, 2H, ArCO), 2.54 (s, 3H, CH_3) ppm, ^{13}C-NMR (DMSO-d_6, 125 MHz) δ 165.9, 160.2, 158.3, 150.6, 145.1, 133.0, 131.0, 129.2, 129.0, 128.9, 127.9, 122.6, 120.7, 21.5 ppm; UV-Vis (e $M^{-1}cm^{-1}$): λ (nm) = 265 (5800), 325 (11,500); HRMS(ESI) m/z $[M+H]^+$: $C_{16}H_{13}N_4O_4^+$, calc: 325.0931; found: 325.0932.

*2.2. Supercoiled Circular pB322 DNA Photocleavage Experiments by QNZs **3a-k**, **4-8**, **11-19***

Compounds were irradiated at various concentrations with UV-Visible light (312 nm−18 W, or 365 nm−18 W, or visible light 400–700 nm−18 W) under aerobic conditions at room temperature for 30 min and in 15 cm distance (312 nm), or 2 h and in 10 cm distance (365 nm

or visible light). Conditions of the photo-biological reaction and gel electrophoresis, quantification of DNA-cleaving activity and calculation of ss% and ds% damage protocols have been described previously [53]. All experiments were performed at least three times.

2.3. Molecular Docking Studies

Organic compounds were fully optimized at the B3LYP/6-31g* level of theory, as implemented in the Gaussian 09 [66] suite of programs (Revision B.01). The crystal data of the B-DNA dodecamer d(CGCGAATTCGCG)2 (PDB 1D:1BNA) were downloaded from the Protein Data Bank [67]. The docking analysis was performed using the AutoDock Vina program [68]. The DNA was adapted for docking by removing water molecules and polar hydrogens, and Gasteiger charges were added by Autodock 4.2 Tools (ADT) before performing docking calculations. Grid box with a size of 60 × 80 × 114 with 0.375 Å spacing was used to encompass the whole DNA. The rigid docking protocol and 100 runs of the Lamarckian genetic algorithm for searching ligand conformations were performed. PyMOL [69] and LipPlot [70] was used for the representation of the docking results and interactions between DNA and compounds.

3. Results and Discussion

3.1. Synthesis

MWI-assisted synthesis for the production of both 3-amino and 3-amido-QNZ was directed via an isolated intermediate; the 2-methyl-4*H*-benzo[*d*][1,3]oxazin-4-one [11] (for simplicity reasons the molecule within manuscript is referred to as "benzoxazinone" or BNZ). Thus, commercially available anthranilic acids **1a-k** were treated with acetic anhydride under MWI to form the corresponding 2-methyl-BNZs **2a-k**. After filtration of the precipitate and washing with petroleum ether, the compounds were individually dissolved in EtOH and further reacted under MWI with hydrazine hydrate to result 3-amino-2-methyl-QNZ **3a-k**.

The DNA photo-cleavage experiments (vide infra) indicated that the nitro and halogenated derivatives were photo-active. As a result, a sequential reaction was designed to afford the formation of an amide functionality. Thus, 3-amino-QNZs **3c**,**e**,**g**,**i**,**j**, reacted with acetic anhydride under classical thermal conditions to give the corresponding acetamides **4-8**, with compound **4**, which is derived from the non-DNA photo-disrupting frame **3c**, to serve as a reference compound for the examination of any behavioural changes concerning photosensitization.

All combined DNA photo-cleaving results for **3a-k** and for **4-8**, led to the design of the synthesis of 6-R-QNZ arylamide derivatives **9-11**, **12-15** and **16-19** (Scheme 1, R=H, R=Br and R=NO_2, respectively), where the aliphatic group of the amide was replaced by aromatic moieties with variation of the electron properties of the substituents on the aromatic ring of the amide. Here, again, compounds **9-11** as aroyl analogues of **3c** were designed as reference compounds to investigate their behaviour towards light. It has been assumed that a compound derived from **3c**, where R=H and Ar=Ph, which does not contain substituents around its aromatic rings, would be photochemically unreactive and therefore not included in the design. All replacements showed activities that are discussed in terms of molecular affinities and dockings via a structural activity relationship study.

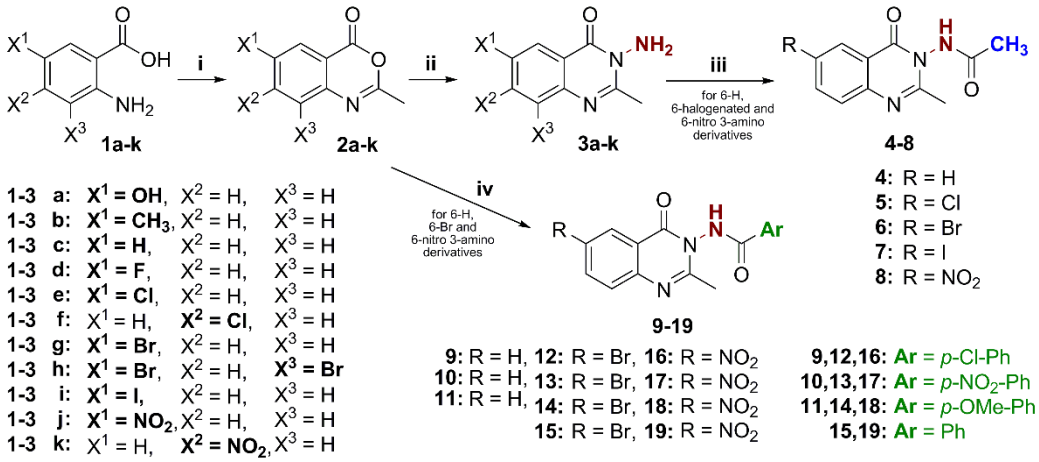

Scheme 1. Reagents and conditions: (i) Ac_2O, MWI (17–22 min), 250 W, T = 120–150 °C, (ii) $N_2H_4{\cdot}H_2O$, EtOH, MWI (20–33 min), 250 W, T = 120–150 °C, 31–85% yield over two steps, (iii) Ac_2O, dry toluene reflux, 12 h, 42–87% yield, (iv) $ArCONHNH_2$, AcOH, MWI (30 min), T = 150 °C, 58–87% yield.

The synthesis of the acetamides **4-8** involved three steps in total, starting from anthranilic acids. For the construction of arylamides **9-19**, a concise two-step protocol under totally MWI conditions, using commercially available inexpensive aryl hydrazides, has been explored. Although not directly related to each other, comparing the reaction times of the final steps, meaning the acetamide thermal formation via the amine (**3** to **4-8**) (12 h) and the MWI assisted arylamide formation via BZN (**2** to **9-19**) (30 min), the new process reduced reaction times about 20-fold and gave no remaining by-products, whereas the use of acetic acid as a reaction solvent made the synthesis of arylamides totally green [71], with the overall yields quite satisfactory.

To the best of our knowledge, neither 3-amino-2-methyl-QNZs nor their derived arylamides have been synthesized entirely under MWI. As a conclusion, the whole synthetic scheme presents an improved methodology for both parent synthone 3-amino-2-methyl-QNZ, as well as for their aroyl derivatives. Compounds **5**, **7-8** and **12-19** are new; therefore, they are properly fully characterized and all their required related data are provided.

3.2. DNA Photocleavage

All compounds were inactive in the dark upon incubation with pBR322 plasmid DNA for 2 h, at their highest concentration. Upon irradiation at 312 nm (UV-B) for 30 min, the majority of the compounds showed photosensitization that led to DNA photo-cleavage, as it was evident at the agarose gel, from the conversion of supercoiled plasmid DNA (Form I) to the nicked plasmid (Form II), and in some cases to the linear plasmid DNA (Form III). Compared to QNZs, which had no substituents on positions 2 and 3 [50] (Figure 1, compounds **VIII**), this set of compounds has four more derivatives demonstrating activity; **3a** (6-OH), **3e** (6-Cl), **3f** (7-Cl) and **3k** (7-NO_2) (Figure 2, lanes 3, 7, 8 and 12, respectively), in addition to the ones which retain activity, meaning those bearing a 6-Br (**3g**), 6,8-di-Br (**3h**), 6−I (**3i**) and 6−NO_2 (**3j**), (Figure 2, lanes 9, 10, 11 and 13, respectively). The auxochromic ability of the OH and, most importantly, of the NH_2 group seems to have contributed to the observed photo-properties. Most profoundly, the hydrogen bonds that appear between the 3-amine group and the DNA bases allow compounds to form a stabilized DNA-compound motif (vide infra) that favour a more efficient attack of the derived reactive oxygen and other radical species towards DNA. Concerning the interaction between DNA and QNZ molecules, the molecular docking studies provided below give a prediction, not evidence, of the real structural state; however, these models highlight several points useful for the discussion.

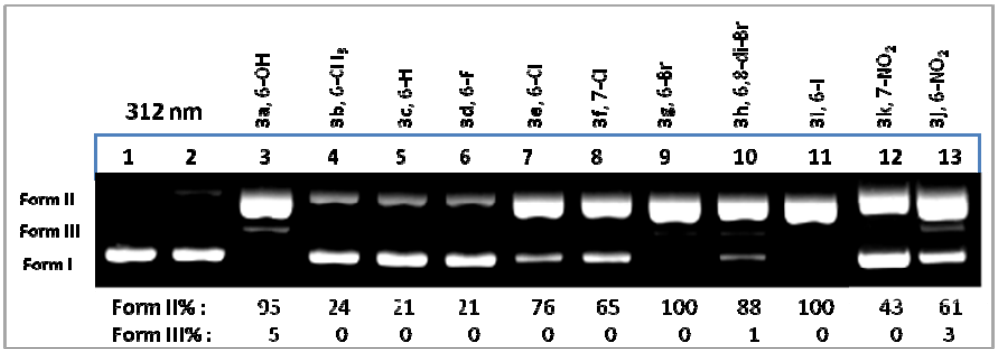

Figure 2. Efficiency on DNA photo-cleavage by QNZ derivatives **3a**-**3j** and **3k** at concentration of 500 μM with UVB light (312 nm). Gel electrophoresis data: Lane 1: DNA without UV irradiation; Lane 2: DNA with UV irradiation; Lanes 3–13: as indicated at the top of the agarose gel.

Under UVA irradiation, DNA photo-cleavage has been observed not only for the two nitro derivatives **3k** and **3j** but also for the hydroxyl and bromo derivative **3a** and **3g** (Figure 3, lanes 12, 13, 3 and 9, respectively). In this series of compounds, in a parallel way to the simple QNZs (**VIII**), the 6-nitro-QNZ derivative was, by far, the most photo-active in this irradiation frame. At 500 μM DNA, photo-disruption was so extensive that ethidium bromide was not able to stain the biomolecule in the agarose gel. 6-Nitro derivatives exhibit better light absorption in the UVA area due, obviously, to the nitro group, which is chromophore. Additionally, as is evident by molecular docking "in silico" calculations, they exhibited better binding affinities towards DNA, creating multiple polar contacts with DNA bases (vide infra). It is noteworthy to mention that many nitro-aromatic derivatives were found in the literature to introduce important photo-physical properties owed to the unique characteristics of the nitro auxiliary [72].

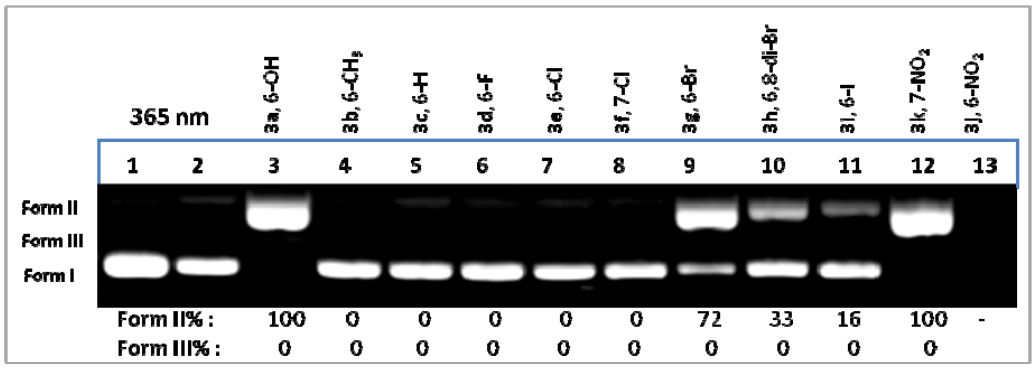

Figure 3. Efficiency on DNA photo-cleavage by QNZ derivatives **3a**-**3j** and **3k** at concentration of 500 μM with UVA light (365 nm). Gel electrophoresis data: Lane 1: DNA without UV irradiation; Lane 2: DNA with UV irradiation; Lanes 3–13: as indicated at the top of the agarose gel.

In order to investigate the capacity of 3-amino-2-methyl-6-nitro-quinazolinone **3j** to photo-cleave DNA concentration dependence experiments have been performed up to the point where 50% of the plasmid DNA was able to be photo-cleaved. The concentration was found to be between 5 and 10 μM (SI, Figure S1). Comparing the activity of compounds holding the same substituent in different positions, 6- or 7-, it seems that position 6- is more activated (6-Cl and 6-NO_2 derivatives exhibit better activity than 7-Cl and 7-NO_2, respectively). In the series of halogenated compounds, 6-Br and 6-I, substituted QNZ were equally active and more efficient than the F and Cl compounds under UVB irradiation in the order 6-F < 6-Cl < 6-Br ~ 6-I. The insertion of a second halogen atom decreased activity. Again, these results are in parallel with the ones observed for compounds **VIII**, Figure 1 [50].

As far as the mechanism of action concerns, it seems that the 6-halogenated derivative **3g** photo-cleaves DNA with the same efficiency under air and under argon (Figure 2, Lane 9 and Figure 4A, Lane 3, under air and argon, respectively). Thus, it may be assumed that the mode of action under anaerobic conditions involves the homolysis of C-Br bond and the formation of aryl and bromine radicals [50]. We have observed, in a few cases where a bond may be homolysed, that excess DMSO enhances photo-cleavage, possibly facilitating the escape of the radicals from the cage [50,54]. Indeed, DMSO was proved here inappropriate as hydroxyl radical scavenger. Sodium benzoate has been used instead, with the activity to be reduced only slightly (Figure 4, Lane 7).

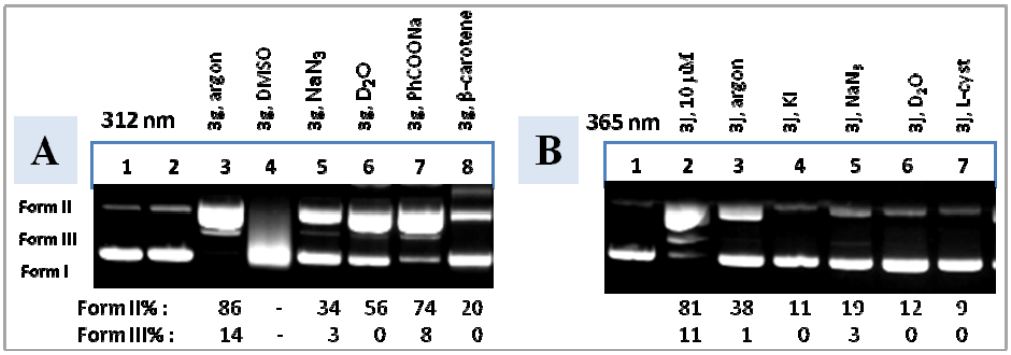

Figure 4. Gel electrophoresis data. (**A**): Mechanistic studies involved at the DNA photo-cleavage by derivative **3g** (500 μM) with UV light (312 nm). Lane 1: DNA without UV irradiation; Lane 2: DNA with UV irradiation; Lane 3: DNA + **3g** + argon; Lane 4: DNA + **3g** + DMSO 20%; Lane 5: DNA + **3g** + NaN_3 20 mM; Lane 6: DNA + **3g** + D_2O; Lane 7: DNA + **3g** + PhCOONa 2 mM; Lane 8: DNA + **3g** + *β*-carotene 200 μM. (**B**): Mechanistic studies involved at the DNA photo-cleavage by derivative **3j** (10 μM) with UV light (365 nm). Lane 1: DNA with UV irradiation; Lane 2: DNA + **3j**; Lane 3: DNA + **3j** + argon; Lane 4: DNA + **3j** + KI 250 μM; Lane 5: DNA + **3j** + NaN_3 20 mM; Lane 6: DNA + **3j** + D_2O; Lane 7: DNA + **3j** + *L*-cysteine 1.5 mM.

On the contrary, the reduction in activity under aerobic conditions in the presence of NaN_3 indicated that singlet oxygen formation is a parallel mechanistic pathway that is involved. Further proof might be the reduction of activity via a triplet state and singlet oxygen quencher such as *β*-carotene [73] (Figure 4A, Lanes 5 and 8, respectively). For the 6-nitro derivative **3j**, the presence of oxygen is, obviously, imperative, since under argon the reaction rate has been reduced and all scavengers disabled DNA photo-disruption (Figure 4B). All these results are quite similar with the ones obtained from simple 6-nitro-quinazolinone [50] and most probably verify a facile Intersystem Crossing to triplet state of nitro aromatic compounds [74].

The first screening for the acetamides **4**-**8** at 365 nm indicated that acetamide **4** was unable to photo-disrupt DNA similarly to its parent compound **3c**. The bromo derivative **6** continued to be active at 312 nm; however, it was inactive under UVA irradiation while its parent compound was active (Figures 2 and 3, **3g**, Lane 9). On the contrary, nitro-derivative **8** retained its full capacity under both irradiation frames (data not shown). Amongst aryl-hydrazides **9**-**11**, the 4-nitro-benzoyl derivative **10** showed very good photo-cleavage activity at 500 μM upon irradiation at 312, as well as at 365 nm (SI, Figure S2). Both 4-Cl and 4-OCH_3 (**9** and **11**, respectively) were inactive. For the 6-bromo aryl-hydrazides **12**-**15**, activity was reduced compared to the parent compound **3g** at 312 nm, and almost disappeared at 365 nm (SI, Figure S2). However, all nitro-derivatives were very active under both irradiation frames, at 500 μM (SI, Figure S2). A concentration dependence DNA photo-cleavage was performed and is shown in Figure 5.

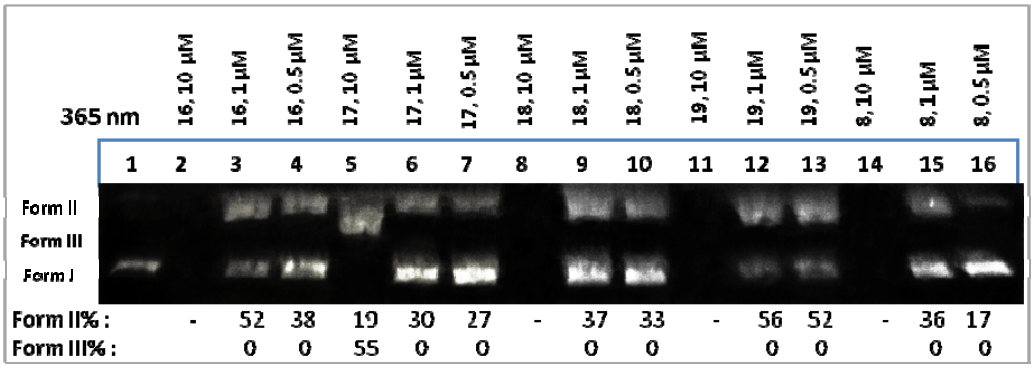

Figure 5. Agarose gel electrophoresis data. Concentration dependence DNA photo-cleavage of compounds **16**–**19** and **8** at 0.5, 1 and 10 μM.

For compounds **16** and **19**, the concentration that photo-disrupted 50% of DNA was around 1 μM, whereas for all compounds, the photo-cleavage was overexpressed at 10 μM, meaning that all compounds seem to be slightly more powerful than their parent compound **3j**.

3.3. DNA Molecular Docking Studies

Molecular docking studies for all non-substituted on the aromatic ring derivatives (Group A: **3c**, **4** and **9**–**11**), all 6-bromo derivatives (Group B: **3g**, **6** and **12**–**15**), as well as all 6-nitro compounds (Group C: **3j**, **8** and **16**–**19**), have been performed. In Tables 1–3, all calculated energy binding values, in addition to DNA base interactions, are provided.

Table 1. Energy binding calculations towards DNA "in silico" of Group A.

A/A	No	Compound Text Representation [a]	E Binding (kcal/mol)	Polar Contacts (PyMOL)	Interactions (LigPlus)
Group A (6-H)	**3c**	**6-H**-QNZ-**3-NH$_2$**	−6.7	DG16, DC15, DG10, DC11	nc [b]
	4	**6-H**-QNZ-**3**-NH**COMe**	−7.1	DG16, DG10, DC11	nc [b]
	9	**6-H**-QNZ-**3**-NH**COAr-Cl**	−9.0	DG16, DG10	nc [b]
	10	**6-H**-QNZ-**3**-NH**COAr-NO$_2$**	−9.4	DA5, DG4, DG22	**HB**: DG4(A) (4−C=O) **VdW**: DA5(A) (4−C=O), DA6(A), DC21(B), DG22(B), DC23(B)
	11	**6-H**-QNZ-**3**-NH**COAr-OMe**	−9.3	DG16, DG10	nc [b]
	-	**6-H**-QNZ-**3**-NH**COAr-H**	−8.8	DG4, DA5, DG22	nc [b]

[a] A text representation of the structure of the molecules is provided for the better comparative reading of the data. It is based on the differentiated structural groups and elements, keeping the central common motif intact under the name QNZ. **6-H**-QNZ refers to the non-substituted derivative on the aromatic ring, **3**-NH**COAr-Cl** represents the *p*-C_6H_4-Cl etc, and **3**-NH**COAr-H** represents the *p*-C_6H_5. The same logic applies to all structural representations. Compounds indicated in green are the ones which exhibited experimentally DNA photo-cleavage; [b] nc: not calculated. **HB**: Hydrogen Bond, **VdW**: Interactions Van der Waals.

Table 2. Energy binding calculations towards DNA "in silico" of Group B.

A/A	No	Compound Text Representation [a]	E Binding (kcal/mol)	Polar Contacts (PyMOL)	Interactions (LigPlus)
Group B (6−Br)	3g	6-Br-QNZ-3-NH_2	−7.0	DG16, DC15, DG10, DC11	**HB**: DG10(A) (4−C=O, 3−NH_2), DG16(B) (4−C=O), DC15(B) (3−NH_2) **VdW**: DC11(A), DC17(B), DG12(A)
	6	6-Br-QNZ-3-NHCOMe	−7.8	DC3, DG4, DA5, DG22	**HB**: DG4(A) (4−C=O), DG22(B) (Me−C=O) **VdW**: DA5(A) (4−C=O), DC23(B), DA6(A), DT7(A) (Br), DC21(B)
	12	**6-Br-**QNZ-**3-**NH**COAr-Cl**	−9.2	DG10, DC11	nc [b]
	13	**6-Br-**QNZ-**3-**NH**COAr-**NO_2	−9.6	DG10, DC11	**HB**: DG10(A) (4−C=O) **VdW**: DA18(B), DA17(B), DC11(A), DG12(A), DG16(B), DG14(B), DC15(B) (Ar−NO−O)
	14	**6-Br-**QNZ-**3-**NH**COAr-OMe**	−9.4	DG16, DC9	nc [b]
	15	**6-Br-**QNZ-**3-**NH**COAr-H**	−8.9	DG10, DC11	nc [b]

[a] A text representation of the structure of the molecules is provided for the better comparative reading of the data. It is based on the differentiated structural groups and elements, keeping the central common motif intact under the name QNZ. **6-H-**QNZ refers to the non-substituted derivative on the aromatic ring, **3-**NH**COAr-Cl** represents the *p*-C_6H_4-Cl etc, and **3-**NH**COAr-H** represents the *p*-C_6H_5. The same logic applies to all structural representations. Compounds indicated in green are the ones which exhibited experimentally DNA photo-cleavage; [b] nc: not calculated. **HB**: Hydrogen Bond, **VdW**: Interactions Van der Waals.

Table 3. Energy binding calculations towards DNA "in silico" of selected groups of compounds. Group C.

A/A	No	Compound Text Representation [a]	E Binding (kcal/mol)	Polar Contacts [b] (PyMOL)	Interactions (LigPlus)
Group C (6-NO_2)	3j	6-NO_2-QNZ-3-NH_2	−7.6	DG16, DC15, DG10, DC11	**HB**: DG10(A) (4−C=O, 3−NH_2), DG16(B) (4−C=O), DC15(B) (3−NH_2), DC11(A) (3−NH_2) **VdW**: DG12(A), DA17(B), DA18(B), [DC21(B), DT7(A), DA6(A) (6−NO−O)], (6−NO−O)
	8	6-NO_2-QNZ-3-NHCOMe	−8.8	DG4, DA5, DA6, DG22	**HB**: DG4(A) (4−C=O) **VdW**: DC23(A) (Me−C=O), DG22(B), [DC21(B), DT7(A), DA6(A) (6−NO−O)], DA5(A) (4−C=O)
	16	6-NO^2-QNZ-3-NHCOAr-Cl	−9.8	DG16, DG10, DC11	**HB**: DG16(B), DG10(A) **VdW**: DC11(A), DG12(A), DG14(B), DC15(B), DA17(B), DA18(B)
	17	6-NO_2-QNZ-3-NHCOAr-NO_2	−10.1	DG2, DG4, DG22	**HB**: DG2(A) (6−NO−O), [DG4(A), DG22(B) (4−C=O)] **VdW**: DC3(A) (6−NO−O), DA5(A), DA6(A), DC21(B) (6−NO−O)
	18	6-NO_2-QNZ-3-NHCOAr-OMe	−10.0	DG16, DG10, DC11	nc [b]
	19	6-NO_2-QNZ-3-NHCOAr-H	−9.5	DG16, DG10, DC11	nc [b]

[a] A text representation of the structure of the molecules is provided for the better comparative reading of the data. It is based on the differentiated structural groups and elements, keeping the central common motif intact under the name QNZ. **6-H-**QNZ refers to the non-substituted derivative on the aromatic ring, **3-**NH**COAr-Cl** represents the *p*-C_6H_4-Cl etc, and **3-**NH**COAr-H** represents the *p*−C_6H_5. The same logic applies to all structural representations. Compounds indicated in green are the ones which exhibited experimentally DNA photo-cleavage; [b] nc: not calculated. **HB**: Hydrogen Bond, **VdW**: Interactions Van der Waals.

In order to better understand the conformational preference of the compounds within DNA, a 3D (by PyMOL), as well as a 2D (by LigPlus), calculation program has been utilized. Although the 3D representation clearly identified all polar contacts with both DNA strands, the 2D offered the hydrogen bonds, as well as additional Van der Waals affiliations, thus allowing a more extensive vision frame for the interpretation of the results.

Evaluating the calculating energies by each group, one may note, based on the binding energy values, the compounds that are predicted to exhibit better DNA photo-cleavage, taking into account only non-covalent interactions and electrostatic factors. Amongst all groups of compounds, the ones bearing the *p*-nitrobenzamido group seem to give the best

perspectives. Indeed, in Group A better energy is observed by compound **10**, in Group B by compound **13** and finally, in Group C the better E binding was found in compound **17**, with the latter to be the best. As far as their experimental photo-cleavage activities are concerned, for Group A, compound **10** not only exhibited the higher energy, but was actually the only photo-active compound within the group (experimentally found photo-activity towards DNA is indicated with green colour in Tables). For Group B, the better binding energy is not translated into enhanced photo-activity, whereas, regardless of the value of the calculated energies, all compounds of Group C were highly photo-active, giving 50% of plasmid photo-cleavage in the range of ~1–5 μM. A common feature we observe amongst photo-responding compound **10** and all compounds of Group C is the nitro auxiliary. As it is known in the literature, in addition to their chromophoric properties, nitro aromatic compounds seem to facilitate the appearance of photo-physical properties able to allow such behaviours [72,74]. However, the case of compound **13** in Group B shows clearly that the existence of only the nitro aromatic auxiliary is not, exclusively, the only demanded condition.

In general, one has to consider that DNA photo-cleavage is a complex phenomenon that requires not only a good affinity to DNA in order for the photo-derived radicals to attack DNA, but also an efficient Intersystem Crossing to the triplet state of the photosensitizer, which is a physico-chemical property of each individual compound.

In order to gain a better structural overview, in Figure 6, molecular dockings for **3c**, **3g** and **3j** (recorded in Tables) are depicted ((**a**), (**b**) and (**c**), respectively). A network of hydrogen bonds owed to QNZ 4−C=O and 3−NH_2 of these compounds appear and, although the formation of the NHCO moiety allows other hydrogen bonds and polar interactions to arise via the acetamide carbonyl or the remaining NH [Figure 7, 4, 6 and 8 ((**a**), (**b**) and (**c**), respectively)], these factors were not the only prerequisite for exhibiting photo-reactivity. It seems that the existence of the free amine functionality is preferable for the majority of the derivatives (see Figures 2 and 3 and comments on the acetamide DNA photo-cleavage).

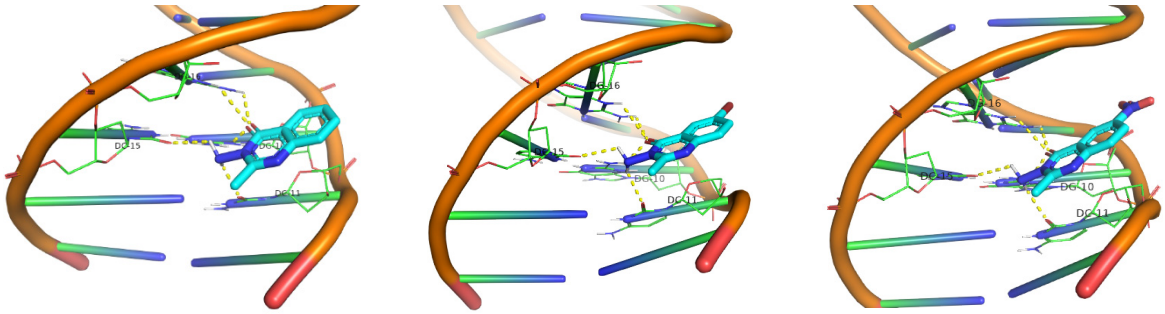

(**a**) (**b**) (**c**)

Figure 6. Panel (**a**): Molecular docking Calculations for compound **3c**; Panel (**b**): Molecular docking Calculations for compound **3g**; Panel (**c**): Molecular docking Calculations for compound **3j**.

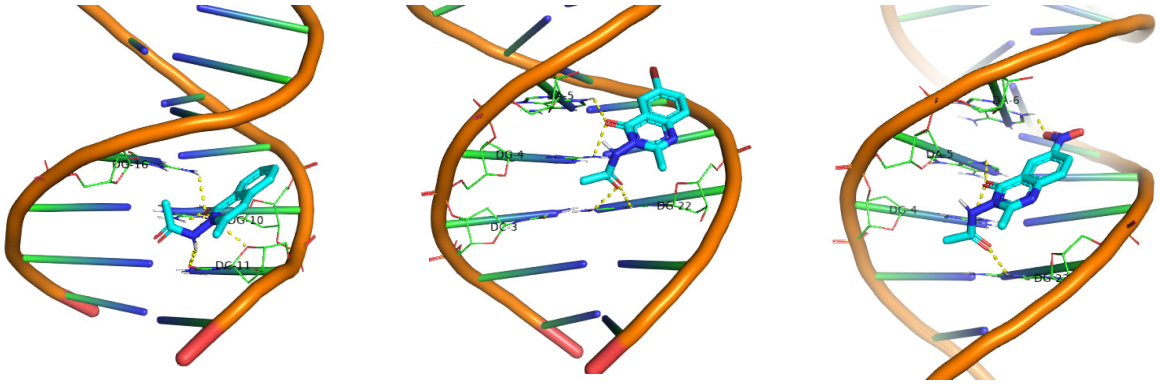

(**a**) (**b**) (**c**)

Figure 7. Panel (**a**): Molecular docking calculations for compound **4**; Panel (**b**): Molecular docking calculations for compound **6**; panel (**c**): Molecular docking calculations for compound **8**.

Interestingly, carefully inspecting all six pictures in Figures 6 and 7, one may observe in Figure 7c, which affords acetamide **8**, that it exhibits an extra interaction involving the 6-nitro group. This compound was found to exhibit very efficient photo-reactivity <<10 μM, (Figure 5). The same 6-nitro group shows DNA interactions, either via hydrogen bond or Van der Waals forces for all 6-nitro-arylamides **16-19** (Figure S5), which exhibited activity in the same range with acetamide **8**. The extra binding efficiency in the distance of the 4−C=O and/or 3-NHCOR functionalities, which are common to all derivatives, obviously offers a better binding affinity and stabilization of the complex DNA compound. Thus, higher calculated binding energies for all compounds of Group C, in relation to their corresponding compounds of Groups A and B, has been observed "in silico". This factor, in conjunction with the photo-properties of the nitro auxiliary, provides this superior DNA photo-disruptive result for compounds in Group C.

In 2D representations of **3g** (Figure 8a), three DNA bases from both strands [DG10(A), DG16(B) and DC15(B)] participate in the hydrogen bonding network with QNZ 4−C=O and 3-NH_2 moieties. In the case of **3j**, four bases participate [DG10(A), DG16(B), DC15(B) and DC11(A)] (Figure 8b), whereas results for both acetamides **6** and **8** (Figure 9a,b), respectively) indicate that they all retain strong interactions. Those findings correlate well with the photo-activities observed by these four compounds.

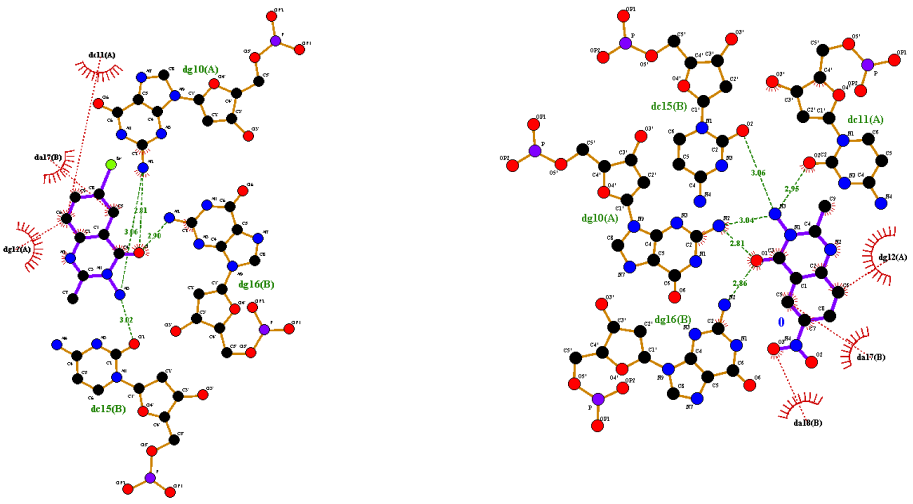

(**a**) (**b**)

Figure 8. Panel (**a**): 2D Molecular Interactions for compound **3g**; Panel (**b**): 2D Molecular Interactions for compound **3j**.

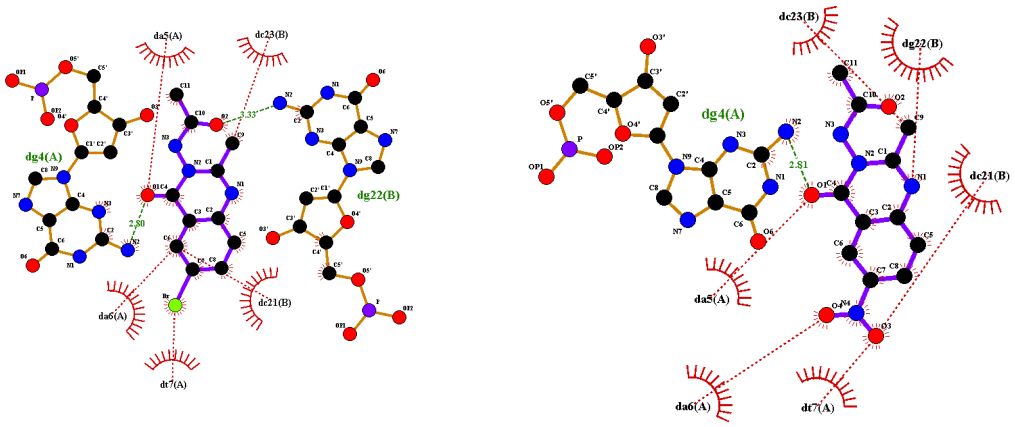

(**a**) (**b**)

Figure 9. Panel (**a**): 2D Molecular Interactions for compound **6**; Panel (**b**): 2D Molecular Interactions for compound **8**.

Finally, the lack of any auxochrome, chromophore or atom with "heavy atom effect" might be the reason for photo-inactivity in the compounds of Group A. However, this QNZ core, in conjunction with an arylamide, has the capacity to form multiple hydrogen bonds (Figure S3) and it is probable that, when joined with a photo-active group, it may serve as an efficient DNA binder and allow DNA photo-cleavage, as in the case of compound **10**.

4. Conclusions

We have synthesized under microwave assisted protocols eleven synthones of the quinazolinone privileged structure, bearing two functionalities on positions 2 and 3; a methyl and an amine reactive group, respectively. The existence of chromophores and auxochromes, such as NO_2, OH and NH_2 groups, facilitated DNA photo-cleavage behaviour for several of those compounds with a variety of aerobic and anaerobic mechanisms of action. More specifically, 3-amino-6-bromo-2-methyl QNZ (**3g**) was active under anaerobic conditions, probably indicating a tendency to homolyse its Br-C bond and form Br· and aryl radicals, which exhibit reactivity towards DNA. Additionally, in the presence of oxygen, the same compound was able to act via singlet oxygen formation. 3-Amino-2-methyl-6-nitro QNZ (**3j**) was active only in the presence of oxygen under UVA irradiation in effective concentration ~5–10 μM, showing characteristics of photodynamic action. It was also active under UVB irradiation, with its broad UV irradiation activity attributed to the nitro chromophore, which allows good UV absorption in this area.

Transformation of the amine group to an amide led to a number of derivatives that constitute either an acetyl or an aroyl group. A thermal reaction for the synthesis of the acetamides **4**-**8** via their 3-amino parent compounds has been chosen, which involved three steps in total and a concise two step protocol for the synthesis of arylamides **9**-**19**, using entirely microwave conditions. DNA photo-cleavage experiments of those derivatives indicated, for the 6-bromo QNZ, that, in general, the photo-activity was reduced, especially at the UVA area. On the contrary, all nitro derivatives enhanced their activity upon UVA irradiation, giving effective concentrations of ~1–5 μM. Interestingly, the simple QNZ, which linked a possible photo-active group (compound **10**), was highly efficient under both UVB and UVA irradiation.

"In silico" DNA molecular docking calculations are generally in correlation with the observed results. More specifically, comparing the compounds that bear the same substituent at position 6- (H or Br or NO_2), their 3-amino derivatives showed lower binding energies than their acetamides and arylamides (amine<acetamide<arylamide). Amongst all, 6-nitro derivatives showed better binding energies compared to the bromo or to the non-substituted ones (H < Br < NO_2). All *p*-NO_2-benzylamides had the higher calculated energy amongst the derivatives within each same group. The identification of efficient

binding of the nitro auxiliary, which is located on the 6- position of QNZ, seems to offer a further stabilization of the DNA-compound complex compared to compounds that bear other substituents in this position. This factor, in conjunction with the photo-activity of the nitro-aromatic moiety, probably explains the much higher experimentally DNA photo-disruption of compounds of Group C. Nevertheless, the amine functionality of the simple 3-amino-QNZs was also found to facilitate activities.

Therefore, 3-amino-QNZs and their amides may be efficiently synthesized under microwave irradiation. Substitution, preferably on position 6-, may "turn on" photosensitization activities that, under certain modifications on the 3-amino group, may remain "on" or "turned off". Based on the fact that QNZs are known for their anticancer and antimicrobial activities, this information might be valuable for the design of novel drugs able to act as photo-chemo or photodynamic therapeutics for cancer photo-treatment and bacteria photo-inactivation.

Supplementary Materials: The following supporting information can be downloaded at: https://www.mdpi.com/article/10.3390/pr10020384/s1, Copies of all NMR spectra; Figure S1: Comparative dose measurement results from DNA photo–cleavage by the quinazolinones derivative **3j** with UV light (365nm); Figure S2: Gel electrophoresis picture of DNA photo–cleavage caused by quinazolinone arylamides at 500 μM (312 and 365 nm); Figure S3: Molecular Docking representations for 6-H arylamides **9**, **10** (3D and 2D), **11** and 6-H-QNZ-3-NHCOAr-H; Figure S4: Molecular Docking representations for 6-Br arylamides **12**, **13** (3D and 2D), **14** and **15**; Figure S5: Molecular Docking representations for 6-NO_2 arylamides **16**, **17** (3D and 2D), **18** and **19**.

Author Contributions: Conceptualization, K.C.F.; Data curation, C.M., M.B., A.D. and K.C.F.; Investigation, C.M., M.B., M.-T.P., A.D. and K.C.F.; Methodology, C.M., M.B. and M.-T.P.; Project administration, A.D. and K.C.F.; Resources, A.D. and K.C.F.; Software, C.M.; Supervision, A.D. and K.C.F.; Validation, C.M., A.D. and K.C.F.; Writing—original draft, K.C.F.; Writing—review and editing, A.D. and K.C.F. All authors have read and agreed to the published version of the manuscript.

Funding: This research received no external funding.

Institutional Review Board Statement: Not applicable.

Informed Consent Statement: Not applicable.

Data Availability Statement: Not applicable.

Acknowledgments: M.B. gratefully acknowledges a Scholarship from State Scholarships Foundation (IKY) for part of this work: This research is co-financed by Greece and the European Union (European Social Fund- ESF) through the Operational Programme «Human Resources Development, Education and Lifelong Learning» in the context of the project "Strengthening Human Resources Research Potential via Doctorate Research" (MIS-5000432), implemented by the State Scholarships Foundation (ΙΚΥ). We also owe thanks to M. Kokotou for performing HRMS analyses at the National and Kapodistrian University of Athens. We are really obliged to the editorial board for a free waver of the manuscript.

Conflicts of Interest: The authors declare no conflict of interest.

References

1. He, D.; Wang, M.; Zhao, S.; Shu, Y.; Zeng, H.; Xiao, C.; Lu, C.; Liu, Y. Pharmaceutical prospects of naturally occurring quinazolinone and its derivatives. *Fitoterapia* **2017**, *119*, 136–149. [CrossRef]
2. Mhaske, S.B.; Argade, N.P. The chemistry of recently isolated naturally occurring quinazolinone alkaloids. *Tetrahedron* **2006**, *62*, 9787–9826. [CrossRef]
3. Khan, I.; Zaib, S.; Batool, S.; Abbas, N.; Ashraf, Z.; Iqbal, J.; Saeed, A. Quinazolines and quinazolinones as ubiquitous structural fragments in medicinal chemistry: An update on the development of synthetic methods and pharmacological diversification. *Bioorg. Med. Chem.* **2016**, *24*, 2361–2381. [CrossRef] [PubMed]
4. Auti, P.S.; George, G.; Paul, A.T. Recent advances in the pharmacological diversification of quinazoline/quinazolinone hybrids. *RSC Adv.* **2020**, *10*, 41353–41392. [CrossRef]
5. Mohammadkhani, L.; Heravi, M.M. Microwave-Assisted Synthesis of Quinazolines and Quinazolinones: An Overview. *Front. Chem.* **2020**, *8*, 580086. [CrossRef] [PubMed]

6. Pathak, P.; Shukla, P.K.; Kumar, V.; Kumar, A.; Verma, A. Quinazoline clubbed 1,3,5-triazine derivatives as VEGFR2 kinase inhibitors: Design, synthesis, docking, in vitro cytotoxicity and in ovo antiangiogenic activity. *Inflammopharmacology* **2018**, *26*, 1441–1453. [CrossRef]
7. Sahu, S.K.; Azam, A.; Banerjee, M.; Acharrya, S.; Behera, C.C.; Si, S. Synthesis, characterization and biological activity of 2-methyl-3-aminoquinazolin-4(3H)-ones Schiff bases. *J. Braz. Chem. Soc.* **2008**, *19*, 963–970. [CrossRef]
8. Gao, X.; Cai, X.; Yan, K.; Song, B.; Gao, L.; Chen, Z. Synthesis and Antiviral Bioactivities of 2-Aryl- or 2-Methyl-3-(substituted-Benzalamino)-4(3H)-quinazolinone Derivatives. *Molecules* **2007**, *12*, 2621–2642. [CrossRef]
9. Jafari, E.; Khajouei, M.R.; Hassanzadeh, F.; Hakimelahi, G.H.; Khodarahmi, G.A. Quinazolinone and quinazoline derivatives: Recent structures with potent antimicrobial and cytotoxic activities. *Res. Pharm. Sci.* **2016**, *11*, 1–14.
10. Sawant, S.D.; Sahu, M.; Nerkar, A.G. Quinazolinone Platinum Metal Complexes: In silico Design, Synthesis and Evaluation of Anticancer Activity. *Asian J. Chem.* **2018**, *30*, 2164–2170. [CrossRef]
11. El-Sayed, N.N.E.; Almaneai, N.M.; Ben Bacha, A.; Al-Obeed, O.; Ahmad, R.; Abdulla, M.; Alafeefy, A.M. Synthesis and evaluation of anticancer, antiphospholipases, antiproteases, and antimetabolic syndrome activities of some 3H-quinazolin-4-one derivatives. *J. Enzym. Inhib. Med. Chem.* **2019**, *34*, 672–683. [CrossRef]
12. Su, C.; Liu, X. Synthesis of Novel 4(3H)-Quinazolinones with 1,2,3-Triazoles Moiety Conjugated by Schiff Base. *Asian J. Chem.* **2014**, *26*, 5301–5304. [CrossRef]
13. Raghavendra, N.M.; Thampi, P.; Gurubasavarajaswamy, P.M.; Sriram, D. Synthesis, Antitubercular and Anticancer Activities of Substituted Furyl-quinazolin-3(4H)-ones. *Arch. Pharm.* **2007**, *340*, 635–641. [CrossRef] [PubMed]
14. Raghavendra, N.M.; Thampi, P.; Gurubasavarajaswamy, P.M.; Sriram, D. Synthesis and Antimicrobial Activities of Some Novel Substituted 2-Imidazolyl-N-(4-oxo-quinazolin-3(4H)-yl)-acetamides. *Chem. Pharm. Bull.* **2007**, *55*, 1615–1619. [CrossRef] [PubMed]
15. Xing, Z.; Wu, W.; Miao, Y.; Tang, Y.; Zhou, Y.; Zheng, L.; Fu, Y.; Song, Z.; Peng, Y. Recent advances in quinazolinones as an emerging molecular platform for luminescent materials and bioimaging. *Org. Chem. Front.* **2021**, *8*, 1867–1889. [CrossRef]
16. Bajaj, K.; Srivastava, V.K.; Kumar, A. Newer Substituted Benzoxazepinylquinazolinones as Potent Antipsychotic and Anticonvulsant Agents. *Arzneimittelforschung* **2003**, *53*, 480–485. [CrossRef]
17. Kashaw, S.K.; Kashaw, V.; Mishra, P.; Jain, N.K.; Stables, J.P. Design, synthesis, and potential CNS activity of some new bioactive 1-(4-substituted-phenyl)-3-(4-oxo-2-methyl-4H-quinazolin-3-yl)-urea. *Med. Chem. Res.* **2011**, *20*, 738–745. [CrossRef]
18. Alagarsamy, V.; Murugananthan, G.; Venkateshperumal, R. Synthesis, Analgesic, Anti-inflammatory and Antibacterial Activities of Some Novel 2-Methyl-3-substituted Quinazolin-4-(3H)-ones. *Biol. Pharm. Bull.* **2003**, *26*, 1711–1714. [CrossRef]
19. Ghabrial, S.S.; Gaber, H.M. Dipolar Cycloaddition Reactions with Quinazolinones: A New Route for the Synthesis of Several Annelated Pyrrolo- and Pyridazinoquinazoline Derivatives. *Molecules* **2003**, *8*, 401–410. [CrossRef]
20. Zeydi, M.M.; Montazeri, N.; Fouladi, M. Synthesis and Evaluation of Novel [1,2,4]Triazolo[1,5-c]quinazoline Derivatives as Antibacterial Agents. *J. Heterocycl. Chem.* **2017**, *54*, 3549–3553. [CrossRef]
21. Farag, D.B.; Farag, N.A.; Esmat, A.; Abuelezz, S.A.; Ibrahim, E.A.-S.; El Ella, D.A.A. Synthesis, 3D pharmacophore, QSAR and docking studies of novel quinazoline derivatives with nitric oxide release moiety as preferential COX-2 inhibitors. *MedChemComm* **2015**, *6*, 283–299. [CrossRef]
22. Dinari, M.; Gharahi, F.; Asadi, P. Synthesis, spectroscopic characterization, antimicrobial evaluation and molecular docking study of novel triazine-quinazolinone based hybrids. *J. Mol. Struct.* **2018**, *1156*, 43–50. [CrossRef]
23. Hassanzadeh, F.; Sadeghi-Aliabadi, H.; Jafari, E.; Sharifzadeh, A.; Dana, N. Synthesis and cytotoxic evaluation of some quinazolinone- 5-(4-chlorophenyl) 1, 3, 4-oxadiazole conjugates. *Res. Pharm. Sci.* **2019**, *14*, 408–413. [CrossRef] [PubMed]
24. Fleita, D.H.; Mohareb, R.M.; Sakka, O.K. Antitumor and antileishmanial evaluation of novel heterocycles derived from quinazoline scaffold: A molecular modeling approach. *Med. Chem. Res.* **2013**, *22*, 2207–2221. [CrossRef]
25. Babu, R.R.; Naresh, K.; Ravi, A.; Reddy, B.M.; Babu, V.H. Synthesis of novel isoniazid incorporated styryl quinazolinones as anti-tubercular agents against INH sensitive and MDR M. tuberculosis strains. *Med. Chem. Res.* **2014**, *23*, 4414–4419. [CrossRef]
26. Ponomarev, I.I.; Razorenov, D.Y.; Petrovskii, P.V. Synthesis of poly(pyridazinoquinazolones). *Russ. Chem. Bull.* **2009**, *58*, 2376–2384. [CrossRef]
27. Patel, V.H.; Patel, M.P.; Patel, R.G. Synthesis and Application of Novel Heterocyclic Dyes Based on 11-Amino-3-Bromo-13h-Acenaphtho[1,2-E]Pyridazino[3,2-B]- Quinazoli Ne-13-One. *Heterocycl. Commun.* **2001**, *7*, 599–606. [CrossRef]
28. Maiti, S.; Kim, J.; Park, J.-H.; Nam, D.; Lee, J.B.; Kim, Y.-J.; Kee, J.-M.; Seo, J.K.; Myung, K.; Rohde, J.-U.; et al. Chemoselective Trifluoroethylation Reactions of Quinazolinones and Identification of Photostability. *J. Org. Chem.* **2019**, *84*, 6737–6751. [CrossRef]
29. Fan, W.; Huang, P.; Chen, X. Overcoming the Achilles' heel of photodynamic therapy. *Chem. Soc. Rev.* **2016**, *45*, 6488–6519. [CrossRef]
30. Zhang, J.; Jiang, C.; Figueiró Longo, J.P.; Azevedo, R.B.; Zhang, H.; Muehlmann, L.A. An updated overview on the development of new photosensitizers for anticancer photodynamic therapy. *Acta Pharm. Sin. B* **2018**, *8*, 137–146. [CrossRef]
31. Wang, Y.; Wang, Y.; Wang, Y.; Murray, C.K.; Hamblin, M.R.; Hooper, D.C.; Dai, T. Antimicrobial blue light inactivation of pathogenic microbes: State of the art. *Drug Resist. Updat.* **2017**, *33–35*, 1–22. [CrossRef]
32. Shleeva, M.; Savitsky, A.; Kaprelyants, A. Photoinactivation of mycobacteria to combat infection diseases: Current state and perspectives. *Appl. Microbiol. Biotechnol.* **2021**, *105*, 4099–4109. [CrossRef] [PubMed]

33. Bhardwaj, S.K.; Singh, H.; Deep, A.; Khatri, M.; Bhaumik, J.; Kim, K.-H.; Bhardwaj, N. UVC-based photoinactivation as an efficient tool to control the transmission of coronaviruses. *Sci. Total Environ.* **2021**, *792*, 148548. [CrossRef] [PubMed]
34. Sobotta, L.; Skupin-Mrugalska, P.; Piskorz, J.; Mielcarek, J. Non-porphyrinoid photosensitizers mediated photodynamic inactivation against bacteria. *Dye. Pigment.* **2019**, *163*, 337–355. [CrossRef]
35. Hamblin, M.R.; Abrahamse, H. Oxygen-Independent Antimicrobial Photoinactivation: Type III Photochemical Mechanism? *Antibiotics* **2020**, *9*, 53. [CrossRef]
36. Ovchinnikova, I.G.; Kim, G.A.; Matochkina, E.G.; Kodess, M.I.; Slepukhin, P.A.; Kovalev, I.S.; Nosova, E.V.; Rusinov, G.L.; Charushin, V.N. Synthesis, photochemical and luminescent properties of ortho-hydroxystyrylquinazolinone-linked benzocrown ethers. *J. Photochem. Photobiol. A Chem.* **2018**, *351*, 16–28. [CrossRef]
37. Kim, G.; Ovchinnikova, I.G.; Nosova, E.V.; Rusinov, G.L.; Charushin, V.N. (E)-2-(Hydroxystyryl)-3-phenylquinazolin-4(3H)-ones: Synthesis, photochemical and luminescent properties. *Arkivoc* **2018**, *2018*, 266–277. [CrossRef]
38. Hricovíni, M.; Hricovíni, M. Photochemically-induced anti-syn isomerization of quinazolinone-derived Schiff's bases: EPR, NMR and DFT analysis. *Tetrahedron* **2017**, *73*, 252–261. [CrossRef]
39. Tokura, Y.; Ogai, M.; Yagi, H.; Takigawa, M. Afloqualone Photosensitivity. Immunogenicity of Afloqualone-Photomodified Epidermal Cells. *Photochem. Photobiol.* **1994**, *60*, 262–267. [CrossRef]
40. Fujita, H.; Matsuo, I. Phototoxic potential of afloqualone, a quinazolinone derivative, as determined by photosensitized inactivation of bacteriophage. *Chem. Biol. Interact.* **1987**, *64*, 139–149. [CrossRef]
41. Fujita, H.; Matsuo, I. UV-A induced DNA nicking activities of skin photosensitive drugs: Phenothiazines, benzothiadiazines and afloqualone. *Chem. Biol. Interact.* **1988**, *66*, 27–36. [CrossRef]
42. Iwamoto, Y.; Itoyama, T.; Yasuda, K.; Uzuhashi, T.; Tanizawa, H.; Takino, Y.; Oku, T.; Hashizume, H.; Yanagihara, Y. Photodynamic Deoxyribonucleic Acid (DNA) Strand Breaking Activities of Enoxacin and Afloqualone. *Chem. Pharm. Bull.* **1992**, *40*, 1868–1870. [CrossRef]
43. Zhou, J.; Liu, L.; Pan, Y.; Zhu, Q.; Lu, Y.; Wei, J.; Luo, K.; Fu, Y.; Zhong, C.; Peng, Y.; et al. Asymmetric Difluoroboron Quinazolinone-Pyridine Dyes with Large Stokes Shift: High Emission Efficiencies Both in Solution and in the Solid State. *Chem. A Eur. J.* **2018**, *24*, 17897–17901. [CrossRef]
44. Lazou, M.; Tarushi, A.; Gritzapis, P.; Psomas, G. Transition metal complexes with a novel guanine-based (E)-2-(2-(pyridin-2-ylmethylene)hydrazinyl)quinazolin-4(3H)-one: Synthesis, characterization, interaction with DNA and albumins and antioxidant activity. *J. Inorg. Biochem.* **2020**, *206*, 111019. [CrossRef]
45. Kakoulidou, C.; Gritzapis, P.S.; Hatzidimitriou, A.G.; Fylaktakidou, K.C.; Psomas, G. Zn(II) complexes of (E)-4-(2-(pyridin-2-ylmethylene)hydrazinyl)quinazoline in combination with non-steroidal anti-inflammatory drug sodium diclofenac: Structure, DNA binding and photo-cleavage studies, antioxidant activity and interaction with albumin. *J. Inorg. Biochem.* **2020**, *211*, 111194. [CrossRef]
46. Kakoulidou, C.; Kosmas, V.-R.; Hatzidimitriou, A.G.; Fylaktakidou, K.C.; Psomas, G. Structure and biological profile of transition metal complexes with (E)-4-(2-(pyridin-2-ylmethylene)hydrazinyl)quinazoline. *J. Inorg. Biochem.* **2021**, *219*, 111448. [CrossRef]
47. Kakoulidou, C.; Hatzidimitriou, A.G.; Fylaktakidou, K.C.; Psomas, G. Interaction of manganese(II) with the hybrid molecule (E)-4-(2-(pyridin-2-ylmethylene)hydrazinyl)quinazoline: Structure and biological profile. *Polyhedron* **2021**, *195*, 114986. [CrossRef]
48. Peng, X.-M.; Peng, L.-P.; Li, S.; Avula, S.R.; Kannekanti, V.K.; Zhang, S.-L.; Tam, K.Y.; Zhou, C.-H. Quinazolinone azolyl ethanols: Potential lead antimicrobial agents with dual action modes targeting methicillin-resistant Staphylococcus aureus DNA. *Future Med. Chem.* **2016**, *8*, 1927–1940. [CrossRef]
49. Peng, L.-P.; Nagarajan, S.; Rasheed, S.; Zhou, C.-H. Synthesis and biological evaluation of a new class of quinazolinoneazoles as potential antimicrobial agents and their interactions with calf thymus DNA and human serum albumin. *MedChemComm* **2015**, *6*, 222–229. [CrossRef]
50. Panagopoulos, A.; Balalas, T.; Mitrakas, A.; Vrazas, V.; Katsani, K.R.; Koumbis, A.E.; Koukourakis, M.I.; Litinas, K.E.; Fylaktakidou, K.C. 6-Nitro-Quinazolin−4(3H)−one Exhibits Photodynamic Effects and Photodegrades Human Melanoma Cell Lines. A Study on the Photoreactivity of Simple Quinazolin−4(3H)−ones. *Photochem. Photobiol.* **2021**, *97*, 826–836. [CrossRef]
51. Armitage, B. Photocleavage of Nucleic Acids. *Chem. Rev.* **1998**, *98*, 1171–1200. [CrossRef]
52. Cadet, J.; Mouret, S.; Ravanat, J.-L.; Douki, T. Photoinduced Damage to Cellular DNA: Direct and Photosensitized Reactions. *Photochem. Photobiol.* **2012**, *88*, 1048–1065. [CrossRef]
53. Pasolli, M.; Dafnopoulos, K.; Andreou, N.-P.; Gritzapis, P.S.; Koffa, M.; Koumbis, A.E.; Psomas, G.; Fylaktakidou, K.C. Pyridine and p-Nitrophenyl Oxime Esters with Possible Photochemotherapeutic Activity: Synthesis, DNA Photocleavage and DNA Binding Studies. *Molecules* **2016**, *21*, 864. [CrossRef]
54. Gritzapis, P.S.; Varras, P.C.; Andreou, N.-P.; Katsani, K.R.; Dafnopoulos, K.; Psomas, G.; Peitsinis, Z.V.; Koumbis, A.E.; Fylaktakidou, K.C. p-Pyridinyl oxime carbamates: Synthesis, DNA binding, DNA photocleaving activity and theoretical photodegradation studies. *Beilstein J. Org. Chem.* **2020**, *16*, 337–350. [CrossRef]
55. Peet, N.P.; Sunder, S. Factors Which Influence the Formation of Oxadiazoles from Anthranilhydrazides and other Benoylhydrazines. *J. Heterocycl. Chem.* **1984**, *21*, 1807–1816. [CrossRef]
56. Gavin, J.; Annor-Gyamfi, J.K.; Bunce, R.A. Quinazolin-4(3H)-ones and 5,6-Dihydropyrimidin-4(3H)-ones from β-Aminoamides and Orthoesters. *Molecules* **2018**, *23*, 2925. [CrossRef]

57. Lambeth, J.D.; Ganesh, T.; Smith, S.M. Quinazoline Derivatives, Compositions, and Uses Related Thereto. WIPO Patent WO2012058211A2, 3 May 2012.
58. Vlaovic, D.; Milic, B.L.; Mackenzie, K. Modified procedure for the preparation of 5-nitro-2-furylmethylene diacetate and its use in the synthesis of some novel (5-nitro-2-furyl) azomethines via 5-nitro-2-furaldehyde. *J. Chem. Res.-S* **1989**, *20*. [CrossRef]
59. Wei, W.; Zhu, L.; Zhou, Y.; Li, Z. Synthesis and Bioactivities Evaluation of Novel N-Pyridylpyrazole Derivatives with 1,2,3-Triazole and Quinazolin-4(3H)-one Substructures. *Heterocycles* **2018**, *96*, 1453–1462. [CrossRef]
60. ElZahabi, H.S.; Nafie, M.S.; Osman, D.; Elghazawy, N.H.; Soliman, D.H.; El-Helby, A.A.H.; Arafa, R.K. Design, synthesis and evaluation of new quinazolin-4-one derivatives as apoptotic enhancers and autophagy inhibitors with potent antitumor activity. *Eur. J. Med. Chem.* **2021**, *222*, 113609. [CrossRef]
61. Babu, Y.R.; Bhagavanraju, M.; Reddy, G.D.; Peters, G.J.; Prasad, V.V.S.R. Design and Synthesis of Quinazolinone Tagged Acridones as Cytotoxic Agents and Their Effects on EGFR Tyrosine Kinase. *Arch. Pharm.* **2014**, *347*, 624–634. [CrossRef]
62. Buyuktimkin, S. Quinazolinones. Part 4: Synthesis of 2-methyl-3-(4-oxo-thiazolidin-2-ylidenanimo)-4(3H)-quinazolinone derivatives | Chinazolinone. 4. Mitteilung: Synthese von Derivaten des 2-Methyl-3-(4-Oxo-Thiazolidin-2-Ylidenamino)-4(3h)-Chinazolinons. *Pharmazie* **1985**, *40*, 393–395.
63. Archana, A.; Srivastava, V.K.; Chandra, R.; Kumar, A. Synthesis of potential quinazolinonyl pyrazolines and quinazolinyl isoxazolines as anticonvulsant agents. *Indian J. Chem.* **2002**, *41*, 2371–2375. [CrossRef]
64. Varnavas, A.; Lassiani, L.; Luxich, E.; Zacchigna, M.; Boccù, E. Quinazolinone derivatives: Synthesis and binding evaluation on cholecystokinin receptors. *Farmarco* **1996**, *51*, 333–339.
65. Ibrahim, S.S.; Abdel-Halim, A.M.; Gabr, Y.; El-Edfawy, S.; Abdel-Rahman, R.M. Synthesis and Biological Evaluation of Some New Fused Quinazoline Derivatives. *J. Chem. Res.* **1997**, *27*, 154–155. [CrossRef]
66. Frisch, M.J.; Trucks, G.W.; Schlegel, H.B.; Scuseria, G.E.; Robb, M.A.; Cheeseman, J.R.; Scalmani, G.; Barone, V.; Mennucci, B.; Petersson, G.A.; et al. *Gaussian 09, Revision B.01*; Gaussian, Inc.: Wallingford, CT, USA, 2016.
67. Drew, H.R.; Wing, R.M.; Takano, T.; Broka, C.; Tanaka, S.; Itakura, K.; Dickerson, R.E. Structure of a B-DNA dodecamer: Conformation and dynamics. *Proc. Natl. Acad. Sci. USA* **1981**, *78*, 2179–2183. [CrossRef]
68. Trott, O.; Olson, A.J. Software news and update AutoDock Vina: Improving the speed and accuracy of docking with a new scoring function, efficient optimization, and multithreading. *J. Comput. Chem.* **2010**, *31*, 455–461.
69. DeLano, W.L. *The PyMOL Molecular Graphics System*; Delano Scientific: San Carlos, CA, USA, 2002.
70. Wallace, A.C.; Laskowski, R.A.; Thornton, J.M. LIGPLOT: A program to generate schematic diagrams of protein-ligand interactions. *Protein Eng. Des. Sel.* **1995**, *8*, 127–134. [CrossRef]
71. Tobiszewski, M.; Namieśnik, J.; Pena-Pereira, F. Environmental risk-based ranking of solvents using the combination of a multimedia model and multi-criteria decision analysis. *Green Chem.* **2017**, *19*, 1034–1042. [CrossRef]
72. Chen, M.; Chen, D.; Chou, P. Fluorescent Chromophores Containing the Nitro Group: Relatively Unexplored Emissive Properties. *ChemPlusChem* **2021**, *86*, 11–27. [CrossRef]
73. Scholz, M.; Dědic, R.; Svoboda, A.; Hála, J. TPP and singlet oxygen quenching by carotene in solution. *J. Mol. Struct.* **2011**, *993*, 474–476. [CrossRef]
74. Zobel, J.P.; Nogueira, J.J.; González, L. Mechanism of Ultrafast Intersystem Crossing in 2-Nitronaphthalene. *Chem. A Eur. J.* **2018**, *24*, 5379–5387. [CrossRef]